

## DIPLOMARBEIT

---

# ESTIMATION OF GAS NETWORK LENGTH AND ASSOCIATED COSTS FOR EU-27 AT NUTS 3 LEVEL BASED ON OPEN DATA

---

zur Erlangung des akademischen Grades

**Diplom-Ingenieur**

im Rahmen des Studiums

**Physikalische Energie- und Messtechnik**

eingereicht von

**Bernhard Mayr**

Matrikelnummer 01327387

Ausgeführt an:

Technische Universität Wien

e-think | Zentrum für Energiewirtschaft und Umwelt

Betreuung:

Associate Prof. Dipl.-Ing. Dr.techn. Christoph LEMELL (TU Wien)

Dipl.-Ing. Dr. Andreas MÜLLER (e-think)

Wien, 20.05.2019:

\_\_\_\_\_  
(Verfasser)

\_\_\_\_\_  
(Betreuer)



Die approbierte gedruckte Originalversion dieser Diplomarbeit ist an der TU Wien Bibliothek verfügbar  
The approved original version of this thesis is available in print at TU Wien Bibliothek.

# Affidavit

I declare in lieu of oath, that I wrote this thesis and performed the associated research myself, using only literature cited in this volume. If text passages from sources are used literally, they are marked as such.

I confirm that this work is original and has not been submitted elsewhere for any examination, nor is it currently under consideration for a thesis elsewhere.

I acknowledge that the submitted work will be checked electronically-technically using suitable and state-of-the-art means (plagiarism detection software). On the one hand, this ensures that the submitted work was prepared according to the high-quality standards within the applicable rules to ensure good scientific practice "Code of Conduct" at the TU Wien. On the other hand, a comparison with other student theses avoids violations of my personal copyright.

Bernhard Mayr



Die approbierte gedruckte Originalversion dieser Diplomarbeit ist an der TU Wien Bibliothek verfügbar  
The approved original version of this thesis is available in print at TU Wien Bibliothek.

# Abstract

The European Union follows the objective of becoming carbon-neutral before 2050. To achieve this goal, a high share of fossil energy carriers (mainly coal, oil and natural gas) must be replaced by renewables. Many scenarios have been developed since then, portraying a European Energy System based on renewable technologies. These scenarios envisage a gradual phase-out of the individual fossil energy sources in the order of their CO<sub>2</sub> emissions from the largest to the smallest. Natural gas, which is considered one of the ‘cleanest’ fossil energy sources, should be the last to disappear from the primary energy mix. However, since the Ukraine crisis, the European Union (EU) aims to drastically reduce the import of Russian natural gas for political reasons. Since the supply of natural gas from other sources is very difficult to replace for transport reasons, it will be eliminated from the primary energy mix even more rapidly in the medium term. According to [1], the influence of drastic changes in the amount of gas flowing through Europeans’ gas networks on costs for gas transport and distribution is not fully understood so far. Therefore, this work aims to develop an Open-source Geographic Information System (OGIS) based economic cash flow model that estimates distribution grid length, gas demand and associated distribution costs in the EU.

In the face of low availability of open natural gas network data, the method follows a top-down approach based on OpenStreetMap (OSM) building data and *www.hotmaps-project.eu* data maps which are open-data. The method is applied to Nomenclature of Territorial Units for Statistics (NUTS) 3 regions of the EU-27 for which results of grid length, gas demand and network costs are shown and discussed on an EU-wide basis. Based on the results, further steps to improve the model are suggested. A sensitivity analysis of the developed model shows the influence of the individual input parameters on the results.

In order to calculate the results for 2050, scenario assumptions of comprehensive building stock renovation measures and exchange of heating systems for the building stock are made to meet the EU goals of a carbon-neutral energy system in 2050. The underlying gas demand on country level (NUTS 0) is taken from an ongoing research project [2] and is not within the scope of this thesis. Based on these scenario assumptions and gas demand, the regional (NUTS 3) results on gas demand and network length show a significant decrease until 2050. Further, net present value calculations show increasing gas distribution costs as a result of decreasing gas sales. Without any countermeasures of network operators, network assets are at risk of becoming stranded or devalued in the medium or long term. Considered measures are increasing grid charges and/or decommissioning of individual lines to guarantee the profitability of distribution networks. Further studies are needed to evaluate potential strategies and their impact.



Die approbierte gedruckte Originalversion dieser Diplomarbeit ist an der TU Wien Bibliothek verfügbar  
The approved original version of this thesis is available in print at TU Wien Bibliothek.

# Kurzfassung

Die Europäische Union verfolgt das Ziel, bis zum Jahr 2050 das Energiesystem CO<sub>2</sub>-neutral zu gestalten. Der Einfluss einer drastisch veränderten Gasnachfrage im Vergleich zur aktuellen Situation auf die Kosten des Gastransports und der Gasverteilung wurde jedoch noch nicht ausreichend untersucht [1]. Ziel dieser Arbeit ist daher die Erstellung eines open-source Geographic Information System (GIS)-basierten ökonomischen Cashflow-Modells zur Abschätzung der Verteilnetzlänge, der Gasnachfrage und der damit verbundenen Kosten für die Gasverteilung in der EU.

Erdgasnetzbetreiber unterliegen keiner Veröffentlichungspflicht ihrer Netz-bezogenen Daten. Deswegen verfolgt die Methode einen Top-Down-Ansatz auf der Grundlage von OSM Gebäudedaten und den Karten von *www.hotmaps-project.eu*, welche alle open-data sind. Eine Sensitivitätsanalyse des entwickelten Modells zeigt den Einfluss der einzelnen Eingangsparameter auf die Ergebnisse. Mit der Methode werden NUTS 3 Regionen in der EU-27 untersucht, wobei die Ergebnisse für Gasnachfrage, Gasnetzlänge und Netzkosten interpretiert und diskutiert werden. Basierend auf den Ergebnissen werden Empfehlungen zur weiteren Verbesserungen des Modells gegeben. Eine Sensitivitätsanalyse untersucht den Einfluss verschiedener Eingangsparameter auf die Ergebnisse.

Für die Berechnungen für das Jahr 2050 wurden umfassende Sanierungsmaßnahmen und der Austausch von Heizungsanlagen für den Gebäudebestand angenommen, um die EU-Ziele eines klimaneutralen Energiesystems im Jahr 2050 zu erreichen. Die zugrunde liegende Gasnachfrage auf Länderebene (NUTS 0) stammt aus einem laufenden Forschungsprojekt [2] und ist nicht Gegenstand dieser Arbeit. Basierend auf diesen Szenario Annahmen und der länderspezifischen Gasnachfrage zeigen die Ergebnisse für den Gasbedarf und die Netzlänge auf NUTS 3 Level einen deutlichen Rückgang bis 2050. Eine anschließende Kapitalwertberechnung zeigt steigende Kosten für die Gasverteilung. Ohne Gegenmaßnahmen der Netzbetreiber besteht die Gefahr, dass die Netzanlagen mittel- oder langfristig entwertet werden. In Betracht gezogene Maßnahmen sind die Erhöhung der Netzentgelte und/oder die Stilllegung individueller Leitungen, um die Wirtschaftlichkeit der Verteilungsnetze zu garantieren. Weitere Studien sind erforderlich, um diese möglichen Strategien und ihre Auswirkungen zu bewerten.



Die approbierte gedruckte Originalversion dieser Diplomarbeit ist an der TU Wien Bibliothek verfügbar  
The approved original version of this thesis is available in print at TU Wien Bibliothek.



# Acknowledgements

The work carried out was funded by the Horizon 2020 programme of the European Union within the projects **NEWTRENDS** (Grant agreement ID: 893311) and **PATH2LC** (Grant agreement ID: 892560).

First, I would like to thank my immediate supervisor **Dr. Andreas Müller**, who provided me with helpful comments, new ideas and critical questions from the first idea to the last sentence of this Master's thesis. Through his guidance, I was able to immerse myself in this topic and learned a lot through his constructive feedback.

Moreover, I would like to offer my special thanks to my primary supervisor **Prof. Christoph Lemell** for his helpful support with coding issues and for the final review.

I would also like to thank all the people from **e-think** and the **Energy Economic Group** who actively supported me with critical comments and helpful ideas during the development of the model. I feel very grateful to have been trusted with a substantial task in the work field of the group. Particularly, I enjoyed the high degree of autonomy during the course of my work.

I'm also grateful to my wonderful girlfriend **Jasmin** and my sister **Cornelia**, who have been tirelessly patient in reading the paper and giving me feedback on the content and spelling.

Last but by no means least I want to thank my parents **Maria** and **Walter** and my sisters **Cornelia** and **Magdalena**. Any of this would not have been possible without your endless support throughout the years.



Die approbierte gedruckte Originalversion dieser Diplomarbeit ist an der TU Wien Bibliothek verfügbar  
The approved original version of this thesis is available in print at TU Wien Bibliothek.

# Table of Contents

<b>1</b>	<b>Introduction</b>	<b>1</b>
<b>2</b>	<b>State of the Art</b>	<b>5</b>
2.1	Europe's Goals and related Documents . . . . .	5
2.2	Natural Gas - Transport and Distribution . . . . .	5
2.3	Network Tariffs Regulation . . . . .	6
2.4	Economic Factors of operating a Gas Infrastructure . . . . .	6
2.5	Economic Analysis: Aim and Methods . . . . .	7
2.5.1	Net Present Value Method . . . . .	8
2.5.2	Annuity Method . . . . .	8
2.6	Gas Models . . . . .	9
2.6.1	Fundamentals of Gas Simulation . . . . .	9
2.6.2	Existing economic Gas Models . . . . .	9
<b>3</b>	<b>Material and Methods</b>	<b>11</b>
3.1	General Description of the Model . . . . .	11
3.2	Projection of Final Energy Demand . . . . .	13
3.3	Gas Demand Estimation . . . . .	14
3.3.1	Final Energy Demand covered by District Heating . . . . .	14
3.3.2	Clustering Heat Demand Hectares . . . . .	15
3.3.3	Calculation of Connection Probability . . . . .	18
3.3.4	Gas Demand of NUTS 3 Regions . . . . .	19
3.4	Length Estimation of Gas Networks . . . . .	21
3.4.1	Number of Gas supplied Buildings . . . . .	22
3.4.2	Empirical Model Fit . . . . .	24
3.4.3	Minimum Gas Distribution Length of NUTS 3 Regions . . . . .	25
3.5	Gas Demand and Network Length of the Power generating Sector . . . . .	25
3.6	Network Cost Estimation . . . . .	26
3.6.1	Development of Gas Demand and Network Length . . . . .	27
3.6.2	Calculation of NPV Parameters . . . . .	28
3.7	Scenario Definition . . . . .	30
3.7.1	Scenario Definition for Demand Projection . . . . .	30
3.7.2	Scenario Definition for Network Strategy of Network Operators . . . . .	33
<b>4</b>	<b>Results and Discussion</b>	<b>35</b>
4.1	Results for selected Regions in Austria . . . . .	35
4.1.1	Results of Gas Demand and Network Length Calculation . . . . .	35
4.1.2	Results of Network Cost Calculation . . . . .	36
4.2	Results for EU-27 . . . . .	38
4.2.1	Results of Gas Demand and Network Length Calculation . . . . .	39
4.2.2	Results of Network Cost Calculation . . . . .	42

## TABLE OF CONTENTS

---

4.2.3	Allocation of potential Gas Distribution Networks . . . . .	45
4.3	Sensitivity Analysis . . . . .	47
4.3.1	Sensitivity Analysis of Network and Demand Estimation . . . . .	47
4.3.2	Sensitivity Analysis of NPV Calculation . . . . .	49
4.4	Validation of Results - Comparison with real Data . . . . .	49
4.5	Model Perspective . . . . .	50
<b>5</b>	<b>Conclusion and Outlook</b>	<b>53</b>
5.1	Modelling . . . . .	53
5.2	Results and future Profitability . . . . .	53
	<b>Appendices</b>	<b>55</b>
<b>A</b>	<b>Standard Values</b>	<b>57</b>
	*	

# List of Abbreviations

- CAPEX** Capital Expenditures
- CM** Calculation Module
- CMs** Calculation Modules
- CP-ID** Construction Period Identification Number
- CRF** Capital Recovery Factor
- DBSCAN** Density-Based Spatial Clustering of Applications with Noise
- DVGW** Deutscher Verein des Gas- und Wasserfaches
- ENTSOG** European Network of Transmission System Operators for Gas
- EU** European Union
- GPN** Gas Demand per Network Length
- Gas20** scenario with connection rate of 20% in 2050
- Gas60** scenario with connection rate of 60% in 2050
- GHG** Greenhouse Gas
- GIS** Geographic Information System
- IPCC** Intergovernmental Panel on Climate Change
- JRC-DB** JRC Open Power Plants Database
- LNG** Liquid Natural Gas
- MRBVF** Mean Rest Booking Value Factor
- MST** Minimum-Spanning-Tree Problem
- NPV** Net Present Value
- NUTS** Nomenclature of Territorial Units for Statistics
- OGIS** Open-source Geographic Information System
- OPEX** Operational Expenditures
- OSM** OpenStreetMap
- WACC** Weighted Average Costs of Capital



Die approbierte gedruckte Originalversion dieser Diplomarbeit ist an der TU Wien Bibliothek verfügbar  
The approved original version of this thesis is available in print at TU Wien Bibliothek.

# Chapter 1

## Introduction

In the 6<sup>th</sup> report of the Intergovernmental Panel on Climate Change (IPCC) scientists renewed and intensified their warning of a global climate crisis if the climate goals of the Paris Agreement are not met in the near future [3]. In November 2018 the European Commission released the report ‘A Clean Planet for all – A European strategic long-term vision for a prosperous, modern, competitive and climate neutral economy’ [4], where the EU proposes pathways of how to reach the target of a climate-neutral economy. The in-depth analyses of the pathways [5] define several scenarios, that consider an 80 %-100 % Greenhouse Gas (GHG) reduction until 2050. In most of the developed scenarios natural gas plays a key role in the transition of the energy system. From 2015 until 2030, the EU’s gross inland consumption share of natural gas is decreasing slowly from 21 % to 20 %. Its further development strongly depends on the GHG emission reduction target and is foreseen to reach 3 % to 9 % in 2050. While assessing other studies, a mixed picture emerges about the role of natural gas in 2050. The range goes from a share of 19 % in the primary energy demand in the Equinor Renewal scenario [6], 15 % in the Shell Sky scenario [7], 10 % in the IEA ETP B2DS scenario [8] and 1 % in the Öko-Vision scenario [9].

Currently, the building sector in the EU holds the biggest share of natural gas gross inland consumption of around 37 %, followed by the power sector of around 32 %. The industry holds a share of 21 %. The transport sector and the ‘non-energetic-use’ sector hold a marginal share of around 5 % [10]. To achieve climate targets, the share of natural gas demand has to decline in each sector. Trends foresee a decrease in the power sector from 16 % in 2015 to 12 % in 2030 and a share between 1 % to 5 % in 2050. In the building sector the share of natural gas decreases from currently 32 % to 31 % in 2030 and show values between 12 % to 23 % in 2050. Studies that see the energy system fully based on renewables make no longer use of natural gas [5].

Depending on the scenario, the individual results of the studies vary with respect to the role of natural gas in the future energy system. However, all studies agree to a decreasing share of natural gas within the EU’s primary energy supply in the next thirty years. Therefore, the role of natural gas infrastructure may also change substantially. At present, the natural gas infrastructure serves to balance the electricity generation and supplies energy to many applications for final energy consumption. The natural gas infrastructure is characterised by high investment costs, a long service time, the need for predictable levels of demand and a high planning certainty provided by the regulatory framework. Looking at the predicted natural gas demand in the future energy system, the business model of network owners and it’s resulting economic profitability is challenged. Generally, a gas bill for individual customers typically consists of 23 % energy price and 35 % network

price [11]. If network prices are kept at the same level, revenues for network operators would decrease because of decreasing demand, whereby investment costs could not be refinanced. Therefore, network costs would have to be adjusted, which in turn would increase gas prices for the individual customers. If there are other heating technology alternatives, more and more customers tend to leave the network. The total costs for remaining customers would increase even further, leading to a spiral of high grid costs and therefore high customer prices which will again cause additional customers to leave the network. A wide variety of scenarios have been developed, which try to identify key findings on the future development of gas infrastructure, to avoid assets, either existing or planned, could become devalued or stranded in the medium or long term [11].

Replacing natural gas with synthetic methane or hydrogen based on renewable resources seems attractive. This option has some advantages, as it makes further use of existing infrastructure, additionally could balance the electricity system and can further increase the security of supply. Especially studies with a stricter GHG emission target show the importance of green gases in a decarbonised future energy system, as shown in Figure 1.1.

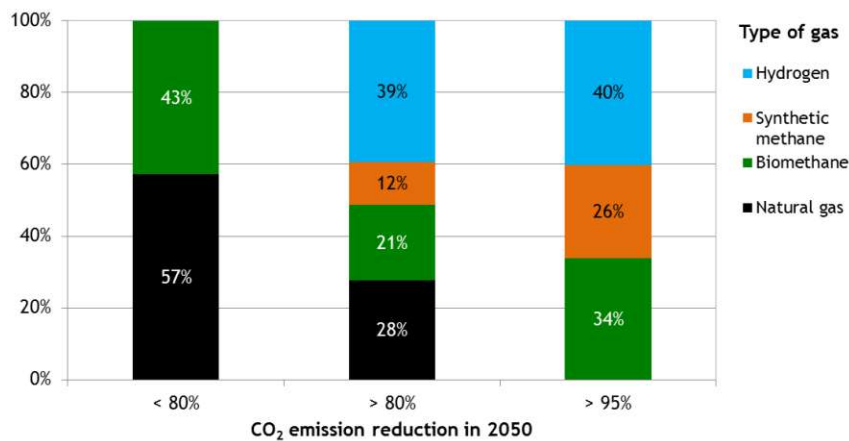


Figure 1.1: Correlation between GHG emission reduction and type of gas until 2050 [11]

Nevertheless, the role of e-methane or hydrogen in the future energy system is very controversial. Most studies agree on a very low hydrogen share (0.1-1.0 %) of the final energy demand until 2030 [12]. However, the studies show a wide diversification in their predictions for 2050. The range goes from 0.2 % to 20 % share in the final energy demand for e-gas and hydrogen. One main reason causes this range: The studies are based on different assumptions about the total final energy demand in 2050. As demand increases, so will the need for alternative energy carriers.

In a German national report [13] a pipeline-based transport of e-fuels is considered indispensable, if the quantity demanded reaches a substantial level. A supply by only on-site electrolyzers is then not possible anymore. However, most of the studies do not at all or just to a little extent consider the costs for gas networks refurbishment and construction [12]. First, transmission network owners have to refurbish parts of their network, making it ready for hydrogen. Furthermore, utilities like gas storage, compressors or valves have to be refurbished or changed too. The costs for long-distance networks refurbishment are seen affordable in most of the evaluated studies [11, 13].

In contrast, the conversion of the distribution network is seen as more difficult. For example, the step-wise change from natural gas to hydrogen supply is not possible, as all



---

the decentral heating and cooking utilities cannot manage a high amount of hydrogen in the fuel mix. The Deutscher Verein des Gas- und Wasserfaches (DVGW) assumes that a hydrogen admixture of 20 % by volume is possible for 80 % of the heating systems in Germany [14]. Considering the lower calorific value of hydrogen, 20 % gas replacement by hydrogen provides just 7 % replacement in calorific value. Above the threshold, a full network refurbishment to 100 % hydrogen has to be accomplished, including all the heating and cooking devices of the end consumers. New types of gas boilers are currently being developed that can be operated with hydrogen and natural gas. If planned in advance, a step-wise installation of such boilers would decrease the effort of changing the whole distribution system at once. Another option would be the construction of an entire hydrogen distribution network, which is seen as too expensive in most of the studies [13]. Considering these obstacles could further drastically change the results of the respective scenarios.

Generally, every technology that runs on hydrogen or synthetic gas has to compete with technology that runs on electricity (direct electrification). Direct electrification means the direct use of electricity for an end-use application, like heat pumps. Scientists, stakeholders, analysts and market participants widely agree on the fact, that direct electrification is the cheapest option in sectors of light-duty vehicles, low/mid-temperature industrial heat ( $< 400^{\circ}\text{C}$ ) and space heating [15]. Only in sectors, where the use of electricity is considered to be impossible or too expensive, alternative solutions like the use of hydrogen or synthetic gas might be the option of choice. The Adriane-Report [13] defines so-called “no-regret-options”, where the use of these alternative solutions will bring added value to the energy system and development in these sectors should be pushed forward. The sectors enumerated in the report are the production of primary steel and basic chemicals, long-haul flights and maritime traffic. The use of hydrogen and synthetic gas in other sectors is widely disputed and is mostly determined by the estimated electrification potential [15].

Finally, the role of the existing natural gas infrastructure in the future energy system is hard to anticipate. Its fate is closely linked to the future development and use of hydrogen or synthetic gases and has to be further elaborated. Therefore this work aims at developing an OGIS based economic cash flow gas model, which should support the broad public, scientists and policymakers to elaborate on questions regarding the future of gas infrastructure. The model and its input data are available under an open-source licence. The OGIS-based model estimates the consumption of gas in the building sector and the length of the supplying infrastructure. Both parameters are fed into a network cost estimation module, which derives the Net Present Value (NPV) of distribution networks in the respective NUTS 3 region. The resulting NPV serves as an indicator for the distribution profitability. The whole calculation is driven by assumptions on the future development of renovation rates and the rates of implementing efficiency measures in the building stock. The model was tested by carrying out the calculation on NUTS 3 regions of the EU-27 under two different scenarios. The scenario with connection rate of 20% in 2050 (Gas20) assumes a gas face-out after 2050 and the scenario with connection rate of 60% in 2050 (Gas60) considers a continuation of gas-based heating systems in the building sector after 2050. Results on estimated gas demand, network length and the NPV of each scenario were compared to each other and recommendations on future model development to improve model calculations are given. Finally a future perspective of the model is drawn.

The thesis is split into four parts. The first part (Chapter 2) gives a short overview of the energy-related goals of Europe and related documents. Also, gas-related topics are

discussed like the composition of the infrastructure, economic assessment tools, existing gas models and their objective.

The second part (Chapter 3) covers a description of the methods of the proposed model. First, a general description provides a comprehensive overview of the individual modules, followed by a detailed explanation of the method. The definition of the studied scenarios closes the Chapter.

The third part (Chapter 4) discusses the results. First, the results of two exemplary regions from Austria (Vienna, Graz) are discussed in detail. Further, the results on European wide extent are plotted, discussed and interpreted and based on the results, further recommendations of model improvements are given. The Chapter is also accompanied by a sensitivity analysis to depict the influence of the most important parameters on the results.

Finally, a description of the future version of the model should give an outlook on further developments. The last part (Chapter 5) summarises the thesis.

## Chapter 2

# State of the Art

The following Chapter is intended to provide a brief overview of the topics on which the model is based.

### 2.1 Europe's Goals and related Documents

Under the resolution of the European Green Deal in January 2020 of the European parliament [16] and its legislative execution, the European Climate Law [17], the European Union follows the objective of becoming carbon-neutral by 2050. This climate law includes the ambitious intermediate climate target of at least 55 % reduction of net GHG emissions in 2030 compared to 1990 [18].

As the energy system is responsible for close to 80 % of total GHG emissions in the EU, the Commission proposes to increase the renewable share of the EU's final energy consumption to 40 % and achieve an overall reduction of 36 to 39 % of primary and final energy consumption in 2030. Since then, a large number of studies have been conducted, which elaborated the feasibility of an energy system transition to a carbon-free future in the EU.

### 2.2 Natural Gas - Transport and Distribution

The principal structure of the natural gas network is divided into three pressure levels. After extraction of natural gas from natural gas fields inside or outside Europe, the gas is transported by off- or onshore pipelines to the cross-border transfer station. The typical pressure is 100 to 200 bar and pipe diameters are around 1-1.4 m. Due to pressure losses through pipeline transport (around 0.1 bar/km), compressor stations are necessary each 100 to 200 km. Gas pressure regulating and metering stations connect the individual pressure levels of the gas network. The stations are responsible for metering the gas flow and ensuring an optimal pressure at the following network level.

The next level is the European transmission network. It is operated with a pressure of around 80 to 100 bar under the use of the full capacity with pipe diameters of around 0.35-1.4 m. The differences between demand and supply are regulated by underground storage facilities. The storage facilities are filled in months with low demand. In months with high demand, they are used to cover peak demands. The European transmission network supplies regional distribution grids.

Distribution grids are operated with pressures between 25 mbar up to 4 bar and with diameters from 80 mm to 1.2 m. Storage facilities can be part of a regional distribution

network too [19].

Depending on the use case, the consumers are connected to different pressure levels of the network. Due to the high gas demand, power stations and large-scale industries are connected directly to the transmission network. Smaller industries, commerce, public institutions and private households are connected to the local distribution network.

### 2.3 Network Tariffs Regulation

Typically grid charges make up around 35 % of customer's energy costs for natural gas [11]. In most European countries, the gas supply network is unbundled from the liberal market and therefore network operators form a natural monopoly [20]. In the interest of maximising welfare on a macroeconomic level, network costs should correspond to marginal costs. In reality, the network operators depend on customers and their agreement to pay network charges. This risk is included in the network costs by a return of equity depending on the capital employed [21], raising the grid charges. In an unregulated environment, grid charges could lead to unreasonable network prices. This is where regulation comes into play: Avoiding excessive network costs, achieving fair prices and cost-efficient network tariffs. Generally all regulation models in Europe are based on the four basic models: the 'cost-plus', the 'rate-of-return', the 'price-cap' or the 'revenue-cap' methods [21]. Most European gas networks operate under the 'revenue-cap' regulation, where each network operator is granted a limit to the total amount of revenues that can be earned by operating a gas network. A government agency defines the individual revenue cap based on supply efficiency and quality. The costs are then passed to each customer depending on the grid level [22].

### 2.4 Economic Factors of operating a Gas Infrastructure

The following Section explains the yearly cost factors for operating gas infrastructure, derived from [19]. Generally an investment is the creation of funds for a measure or a project. It begins with an expenditure (investment) and triggers a series of revenues and expenditures over its service time. The individual costs, which are part of the analysis are displayed in Figure 2.1. The yearly costs for gas infrastructure are distinguished into fixed costs and variable costs. The fixed costs are independent of the energy distributed by the network. However, the variable costs depend on the transported energy.

One part of the fixed costs are the *capital costs*, which consist of three parts: The first part consists of depreciation costs. A depreciation is not a real expenditure but is considered for tax reasons in accounting and deprecate investment costs. Interest on borrowed capital is the cost that must be paid for a borrowed amount of money. This includes interest on loans, promissory note loans or bonds. The return on equity takes into account the profitability of the investment calculated by dividing net income by shareholders equity.

Another part of the fixed costs is the *income tax*. The *income tax* takes into account the tax on corporate income and the country-specific trade tax. The last part of the fixed costs are the *consumption independent costs*. These costs take into account the costs for labour, maintenance and other fixed costs for operating the asset. The variable costs consist of *consumption dependent costs* and take into account the variable maintenance costs, costs for operating the assets and costs for product disposal.

All these costs can be divided into Capital Expenditures (CAPEX) and Operational Ex-

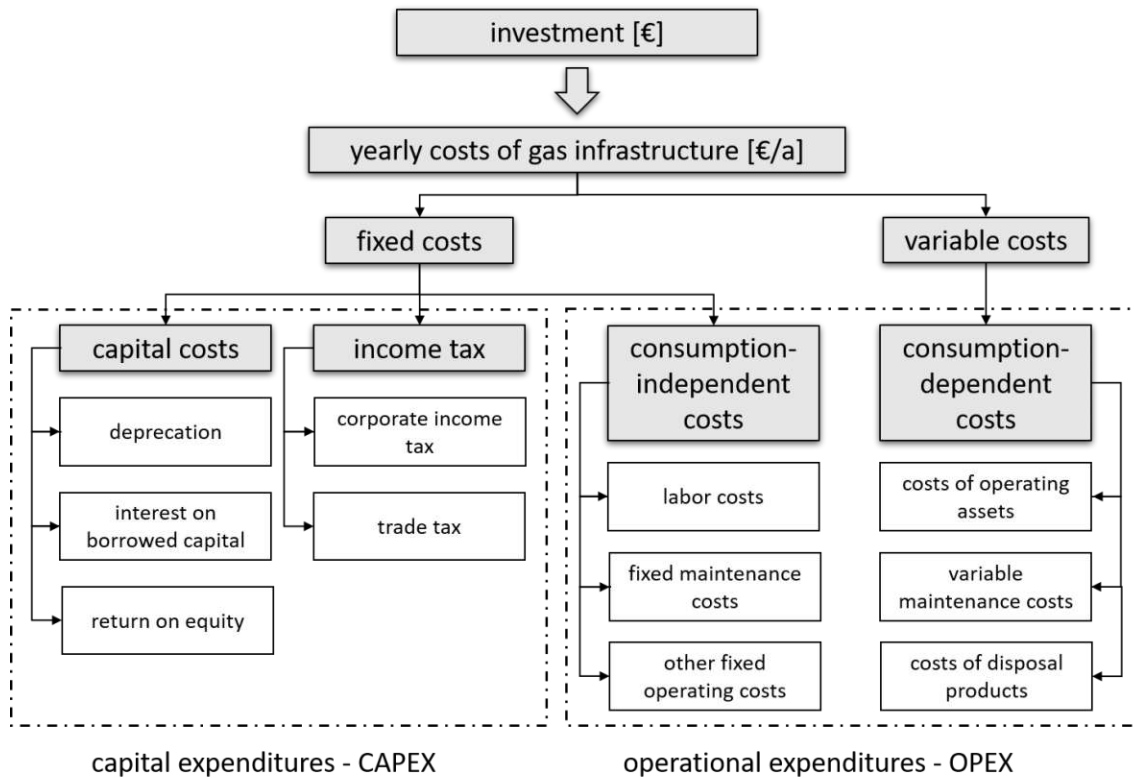


Figure 2.1: Economic factors of operating a gas infrastructure

penditures (OPEX). The CAPEX summarise all expenditures based on the expenditures of the investment. The OPEX are equivalent to the expenses for operating the asset (labour costs, maintenance costs, etc.). The costs which are part of the OPEX or CAPEX are surrounded by the dot-dashed squares in Figure 2.1.

Cost components for the distribution grid in the city of Bamberg are evaluated in [23] and an Equation for the calculation of the yearly revenue cap is derived. Further, the model in [23] consists of an Equation to calculate the OPEX, which is being used in the network cost calculation of this thesis. The OPEX calculation depends on the grid length and supplied energy [23]. The cost components of OPEX calculations are based on an estimation for operational costs, loss costs, upstream grid charges and concession fees.

## 2.5 Economic Analysis: Aim and Methods

The economic analysis aims to assess the absolute and relative efficiency of one or more investment measures. Before an economic analysis is performed, all the investment options are made comparable to each other. By comparing several investment options, the analysis only has to consider expenses and not revenues. If there is only one option, both have to be considered.

In the energy sector, the main purpose of economic analyses is to assess different investment options for energy generation or distribution. Depending on the type of investment, the static- or dynamic procedure for economic analysis is used. Dynamic procedures discount the payment series, static procedures don't. An investment method usually sums up cash flows from different dates and compares them to each other. To make all cash flows comparable, it is necessary to discount each cash flow to a referenced point in time.

Discounting is the method of considering the time-value of money, because not only the value of payment but also the date of maturity is important. Invested money has the ability to earn interest over time. That's the reason, why the value of invested money increases over time because of accumulated interests. For investments with a long duration, such as in the energy industry, the dynamic methods are preferably used. For relatively small investments such as improvement measures, it often makes more sense to calculate statically.

Since the energy sector mostly uses the dynamic procedure is mostly used in the energy sector, its methods are described below in detail. Payment series are discounted or compounded depending on the point in time when the payment is made according to

$$K_n = K_0 \cdot (1 + i)^n = K_0 \cdot q^n \quad , \quad (2.1)$$

where  $K_n$  is the absolute value of an investment in the future, called *nominal value* and  $K_0$  is the absolute value in the present, called *present value*. A payment is discounted according to

$$K_0 = \frac{K_n}{(1 + i)^n} = \frac{K_n}{q^n} \quad . \quad (2.2)$$

The parameter  $q$  describes the compound- or the discount factor and is calculated by the interest rate  $i$  with  $q = (1 + i)$  [19]. The interest rate  $i$ , or Weighted Average Costs of Capital (WACC), is the anticipated rate of return, which is expected from an investment. Its calculation considers, if equity and loans are used, the ratio of equity and borrowed capital, return on equity plus risk of investment, taxes, etc.

### 2.5.1 Net Present Value Method

The method aims to calculate the NPV. It is the balance of all present values of expenditures and revenues within the service time of investment. It is the absolute value an investment makes in addition to the interest rate. If the value is negative, it is more advantageous to invest the investment sum at the calculated interest rate differently (e.g. stocks, savings account). All cash flows, which are made in the future or in the past, are discounted or compounded to a referenced time point. Normally the point in time is defined, when a plant or a system is commissioned. The method follows

$$K_0 = -I_0 + \sum_{t=1}^{t=n} \frac{R_t - E_t}{q^t} \quad , \quad (2.3)$$

where  $K_0$  describes the *present value*,  $I_0$  is the investment at the beginning of the project,  $R_t$  and  $E_t$  are the revenues and the expenses at the end of year  $t$  in euro per year. The factor  $q$  is the discounting factor. If the NPV is positive, an investment is supposed to be cost-efficient. If compared to other options, the investment with the highest NPV is the most cost-efficient.

In this thesis the NPV-method is used to calculate the absolute NPV (revenues and expenditures are considered). To determine if a distribution network is economically profitable or not. The method is explained in detail in Section 3.6.

### 2.5.2 Annuity Method

The annuity method converts all cash flows derived from an investment into equivalent rates of cash flows over its service time. The equivalent rates of cash flows are summed up and the result is called *annual equivalent amount* (annuity). In contrast to the NPV method, the annuity method does not calculate the overall profit, but rather the periodic

profit of an investment. The investment is advantageous if the annuity is positive. If compared to other investment options, only the expenses are considered in the economic assessment. The option with the lowest yearly average cost is the most cost-efficient option. The annuity is calculated by multiplying the present values of all cash flow series by the Capital Recovery Factor (CRF). The factor is defined as

$$\text{CRF} = \frac{1}{\sum_{t=1}^{t=n} \frac{1}{q^t}} = \frac{(1+i)^n \cdot i}{(1+i)^n - 1} \quad , \quad (2.4)$$

where  $t$  is the year of service time and  $n$  is the total service time.

When absolute values of investments are calculated, the annuity method and NPV method lead to the same result. When different investment options are compared to each other the methods can lead to different results.

## 2.6 Gas Models

### 2.6.1 Fundamentals of Gas Simulation

The investigation of how to optimally and economically develop natural gas transport and distribution pipeline networks is a complex task. Therefore the assessment of such complex systems strongly relies on computer-aided simulation procedures. Depending on the use-case, such simulations are generally based on numerical procedures, using basic models of continuum mechanics, numerical methods of mechanics or hybrid methods of mathematical optimisation.

Depending on the gas flow, the simulations can be distinguished into steady-state models or unsteady state models. In steady-state models, time-dependent characteristics like pressure oscillations are not considered. The network system is described by relatively simple algebraic equations, which provide results for a single instant in time. The fundamental equations are derived from Bernoulli's Equation and Kirchhoff's laws [24]. All elements in the network system are assumed to be at constant flow conditions.

Unsteady-state models consider time-dependent characteristics. In some cases, process flow dynamics within the network can not be neglected. Real-world conditions like pressure propagation during opening or closing a valve accounted for in these models. Unsteady-state models are based on partial differential Equations, which are solved by numerical methods [24]. It makes the models more realistic but more complex and more difficult to solve the mathematical system.

### 2.6.2 Existing economic Gas Models

At present, a large number of different gas network models exist. Their objective ranges from allocating gas quantities in a pipeline network, optimising fuel consumption, planning capacities to controlling the network load distribution for the next couple of hours to minimise costs of network assets. They differ in time resolution (year, day, hours) as well as in spatial resolution (transnational, national, regional). This thesis focuses on economic gas models, therefore the next Section will give an overview of existing economic models.

Basically there are two types of gas models: infrastructure-orientated, short-term *dispatch models* and competition-orientated, long-term *market models* [25]. Both types of model approaches are based on the representation of the infrastructure as a node-edge model. A

node-edge model is a mathematical model to represent network-like structures in different scientific disciplines, where the nodes represent objects within the network and edges represent the relations between the objects.

The objective of a *market model* is to simulate a realistic behaviour of the market participants. It considers different players within the market pursuing different goals. The optimisation target follows the revenue maximisation of the different players with market power (network operators, producers, consumers, etc.). Such models allow drawing conclusions in the long-term regarding price development, energy supply security for end consumers, consumer behaviour etc.

*Dispatch models* optimise the gas flow from production to the consumer without consideration of market power on the respective system level. The optimisation target is the minimisation of system costs, following a perfect competition as well as an efficient regulatory approach [25]. Regarding this simplification, the model allows a highly temporal and local resolution of the network, including a realistic representation of the physical gas network and its asset. Such models can help to identify bottlenecks in the transport infrastructure and answer questions regarding network expansion etc.

In [25] current large scale models and their prediction quality of historical price developments, network flows and gas storage levels of German gas storage facilities are evaluated. The article emphasises the fact that such models have great prediction limitations due to unexpected market events. The reason for that are secret contracts between market players, which lead to unexpected behaviours of market players, or events like Fukushima which influence the gas price. Therefore, such models can only show basic relations which result in fundamental conclusions.

Existing models focus often on a large scale. However, gas models with a focus on the regional level exist too. Their objective is to draw conclusions of the future development of network assets in face of decreasing gas demand, or the strategic behaviour of network operators to maximise profit or minimise loss. Such models are typically based on a node-edge approach. Due to their size, it is possible to solve the gas flow within the network system in a high temporal and local resolution. The backbone of such high-resolution models is an adequate piping grid simulation tool. Next to commercial tools, open-source available software, like Pandapipes [26], exists. It simulates steady-state or time-series-steady-state gas flow and allows identification of bottlenecks, critical pressure drops and other malfunctions of the network.

Gas models are as good, as their availability of infrastructure- and consumption behaviour data. Usually, such infrastructure is classified as critical and data about network infrastructure is hardly publicly available. Therefore most studies which tackle questions on a regional level are conducted in cooperation with the local distribution network operator delivering these data.

This thesis focuses on the future of distribution grids in a decarbonised energy system in the EU-27. Due to the poor availability of open-source data, the approach is limited to a basic distribution grid length and gas demand calculation followed by a calculation of associated costs for gas distribution on a regional level.



## Chapter 3

# Material and Methods

This chapter first provides a general description of the model, followed by the method of how the final energy demand is projected into the future. Then it presents the detailed workflow of the gas demand, gas distribution grid length and network costs estimation and finally describes the scenario assumptions.

### 3.1 General Description of the Model

The main objective of the OGIS-based economic cash-flow model is the calculation of gas distribution grid length, gas demand and associated gas distribution costs in selected NUTS 3 regions. Figure 3.1 gives a general overview of the developed model and its workflow. Yellow boxes show data, which serve as input for the model's individual Calculation Modules (CMs). The CMs are shown as grey boxes. Blue boxes indicate interim results, which are input data for the following CMs. The final output is shown as a green box. What follows is a brief description of the individual CMs, the input data, the interim results and the output followed by a more detailed description in Section 3.6.

The model itself consists of four individual calculation modules. The first calculation module (Calculation Module (CM) #1) calculates the length of gas distribution networks in the selected region (Section 3.4). It is based on an empirical model, which provides a functional relation between the minimum pipe length required to connect a set of buildings and the number of buildings per hectare [27]. The number of buildings per hectare or so-called building density raster was generated from the OSM database (input data #1, Figure 3.1) and the open data set from the hotmaps project [28]. The calculated gas distribution length per NUTS 3 region serves as an input for CM #4.

Whether or not an area has a gas infrastructure is assumed to depend on the distance to the next European transmission line. Therefore CM #2 creates a map with a resolution on hectare level ( $100\text{ m} \times 100\text{ m}$ ), where each hectare element contains the distance to the nearest transmission line, in the unit of  $100\text{ m}$  (Section 3.3.3). The raster is derived from the *SciGRID\_gas* map [29], which contains the location of the European natural gas transmission network and its assets. The output of this module is an input for CM #1 and CM #3.

CM #3 calculates the total gas demand in the building sector of the respective region (Section 3.3). The inputs for this module are generated by the open-source demand-projection tool from the hotmaps toolbox [30] (Section 3.2). The demand-projection tool generates a heat density map [28] which indicates the final energy demand for hot water preparation and space heating for the building sector in a selected year. The generated heat density

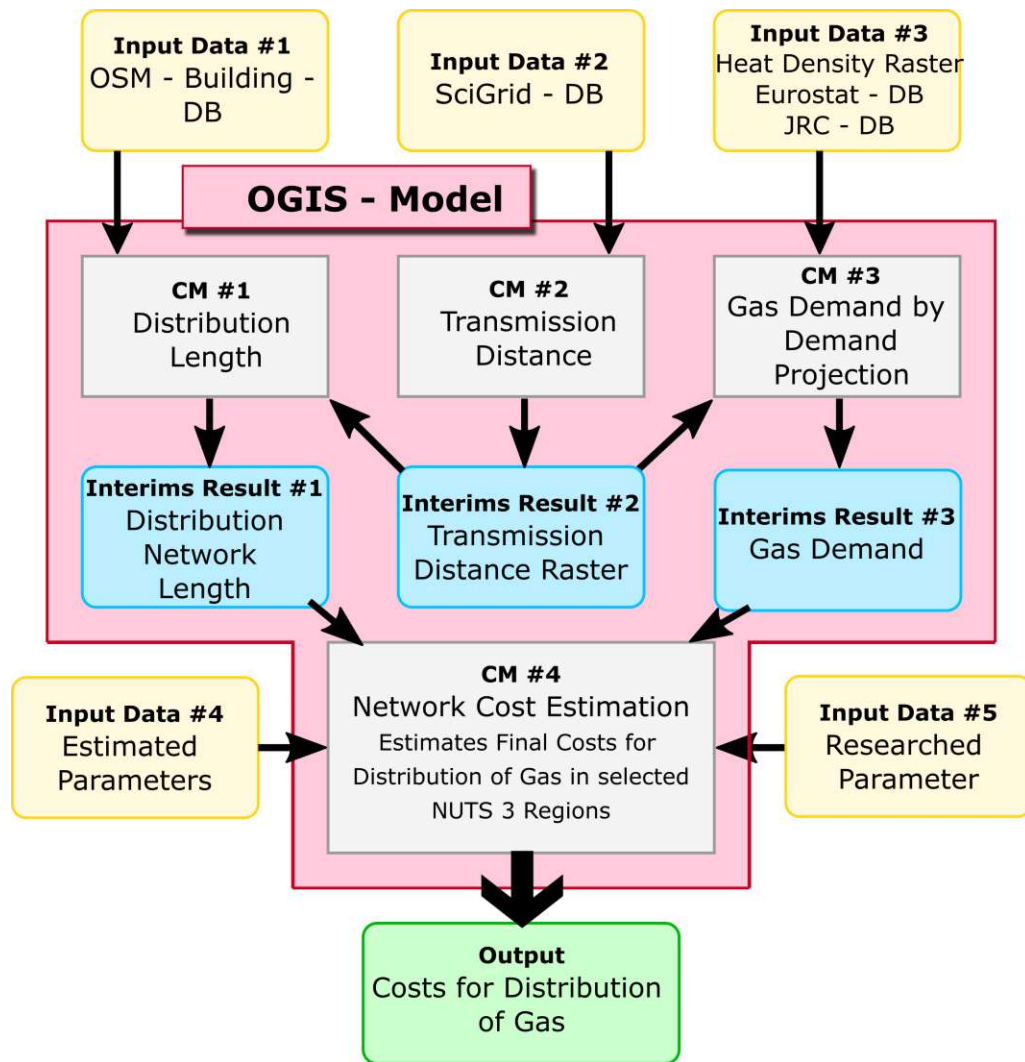


Figure 3.1: General description of the developed OGIS model

map is based on several scenario assumptions (Section 3.7). Further input parameters for CM #3 are parameters, which deliver statistical information like the share of gas heating in buildings in each EU country. The output of the module is the total gas demand of buildings in the selected NUTS 3 region.

Finally CM #4 calculates the gas distribution costs in the selected region. The final cost calculation is based on the Net-Present-Value method (Section 3.3). It calculates the NPV of all distribution grids in a selected NUTS 3 region (Section 3.6). The investment costs for network assets and operational costs are derived from [1]. The module is fed by intermediate results derived from the previous CMs as well as user-defined input parameters and parameters given in scientific literature. The generated output is the NPV for the distribution of gas in the selected NUTS 3 region.

Currently, the OGIS model calculates the gas demand and the length of the supplying network from the building sector, as well as the NPV of the gas distribution networks. According to the energy balances in Eurostat [10] 23 % of the total natural gas consumption in EU-27 is covered by industry, 36 % is covered by the residential and non-residential sectors and 31 % is covered by power and the heat generating sectors. The current model version has no implementation of gas demand and network length estimation for the in-

dustrial sector but already for the power and heat generating sectors. Although the results of this sector are not used in the NPV calculation, the implemented (yet not used) module is presented in this thesis. The current version of the model also does not consider the transport sector. At the moment the consumption of gas in the transport sector in the European Union is negligibly small, but will most likely increase in the long term [11].

### 3.2 Projection of Final Energy Demand

The calculations in this thesis are based on the heat density map (final energy demand for hot water and space heating) from the hotmaps project [28]. This data set shows its data on hectare level for EU-27 plus Norway, Switzerland, UK and Iceland for the year 2015. The generation of the map is based on a statistical approach which correlates the building stock characteristic with final energy demand for space heating and hot water preparation. The process was carried out by a spatial distribution function which distributed available statistical data on national level (NUTS 0) to regional level (NUTS 3). Finally, the same process was applied to infer hectare level data from the NUTS 3 level [28]. The distribution function builds on the central idea, that the demand in the residential and service sectors correlates with population density, climate conditions and economic activities. The developed map is available under the Creative Commons Attribute 4.0 International License which makes it freely usable.

The heat density map shows data for the year 2015. This work aims to generate results on the future costs of gas distribution systems. To make statements on the future development of gas infrastructure, the map needs to be projected into a certain year after 2015 under defined assumptions. This is where the demand-projection tool [30] comes into play: the tool projects the building sector's final energy demand for space heating and hot water preparation into a defined year. It assumes a change of the final energy demand over the years due to three activities:

- A fraction of the buildings gets renovated and the heat demand decreases.
- Another fraction of the buildings is only maintained, the heat demand remains the same.
- The last fraction of the buildings is demolished.

The tool also takes into account newly constructed buildings which increase the heat demand. The rates at which the individual actions happen are defined by certain pre-defined scenario inputs. The scenarios are calculated by using the Invert/EE-Lab module. The module is a dynamic bottom-up techno-economic simulation tool that evaluates the effects of different policy packages on the total energy demand, energy carrier mix, CO<sub>2</sub> reductions and costs for space heating, cooling, hot water preparation and lighting in buildings [31].

Figure 3.2 shows in the left panel the final energy demand for space heating and hot water preparation in 2015. The brighter the colour of the respective hectare element, the higher the final energy demand. The panel on the right shows the projected final energy demand for the year 2050 under the Gas60 scenario. The scenario is explained in detail in Section 3.7. In this example, the final energy demand for space heating and hot water preparation decreases from 2015 to 2050.

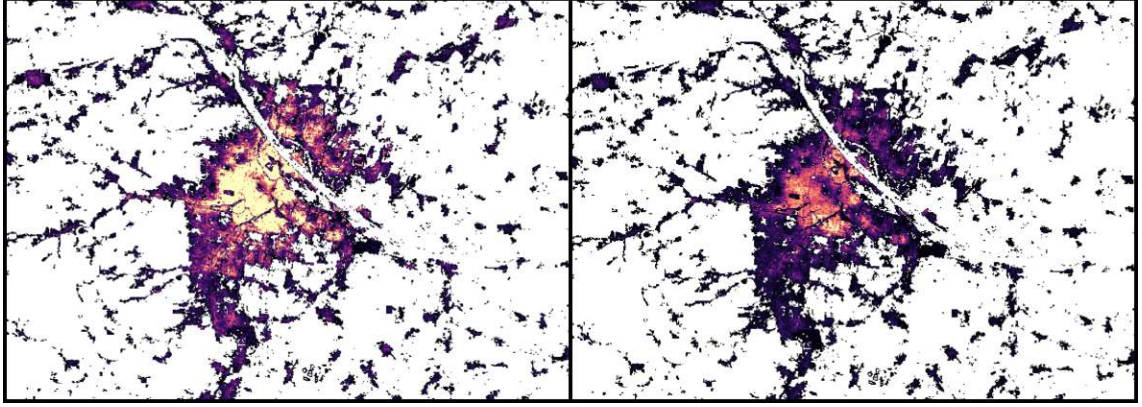


Figure 3.2: Final energy demand of Austrian city of Vienna for 2015 (left) and projected for year 2050 (right)

### 3.3 Gas Demand Estimation

The final gas demand in each NUTS 3 region was derived from the heat density map by first calculating the potential share of district heating from the final energy demand. Second, demand covered by district heating was calculated and subtracted from the final energy demand (Section 3.3.1). Third, the remaining final energy demand out of the map was used to derive a so-called gas share potential  $\text{pot}_{i,j}^{gas}$ , which is the potential share of gas covering the remaining final energy demand for space heating and hot water preparation (without final energy demand covered by district heating). Finally the gas demand for space heating and hot water preparation in each NUTS 3 region was derived from the gas potential (Section 3.3.4).

#### 3.3.1 Final Energy Demand covered by District Heating

To estimate the final energy demand ( $fed$ ) covered by district heating ( $dh$ ) in any given hectare ( $i, j$ ), the following 3-step assumption is made: In a first step, the hectare elements' final energy demand  $h_{i,j}^{fed}$  ( $fed=final\ energy\ demand$ ) that exceeded a user-defined value ( $\text{limit}_{dh}$ ) were assigned to be fully supplied by district heating. In other words, their potential share of district heating from the total final energy demand for space heating and hot water preparation is 1. In a second step, hectare elements' final energy demand below this threshold, district heating supplies a fraction of the total final energy demand, according to

$$\text{pot}_{i,j}^{dh} = \begin{cases} \frac{h_{i,j}^{fed}}{\text{limit}_{dh}}, & \text{for } h_{i,j}^{fed} \leq \text{limit}_{dh} \\ 1, & \text{for } h_{i,j}^{fed} > \text{limit}_{dh} \end{cases}, \quad (3.1)$$

where  $\text{pot}_{i,j}^{dh}$  is the potential share of district heating in hectare ( $i, j$ ). In the third step, the hectare elements' final energy demand covered by district heating  $h_{i,j}^{fed,dh}$  is calculated by

$$h_{i,j}^{fed,dh} = h_{i,j}^{fed} \cdot \text{pot}_{i,j}^{dh} \cdot f^{dis,dh}. \quad (3.2)$$

$f^{dis,dh}$  serves as a scaling factor, to meet the national share  $x^{dh}$  of district heating in the supply mix for space heating and hot water preparation ( $dis=discrepancy$ ). The factor is calculated by

$$f^{dis,dh} = \frac{\sum_{i,j} h_{i,j}^{fed} \cdot x^{dh}}{\sum_{i,j} h_{i,j}^{fed} \cdot \text{pot}_{i,j}^{dh}}. \quad (3.3)$$

The left panel of Figure 3.3 shows the final energy demand for space heating and hot water preparation ( $h_{i,j}^{fed}$ ) for the Austrian city Vienna and the right panel shows the resulting final energy demand covered by district heating ( $h_{i,j}^{fed,dh}$ ) according to Equation 3.2. The brighter the colour appears in the panels, the higher the demand for final energy.

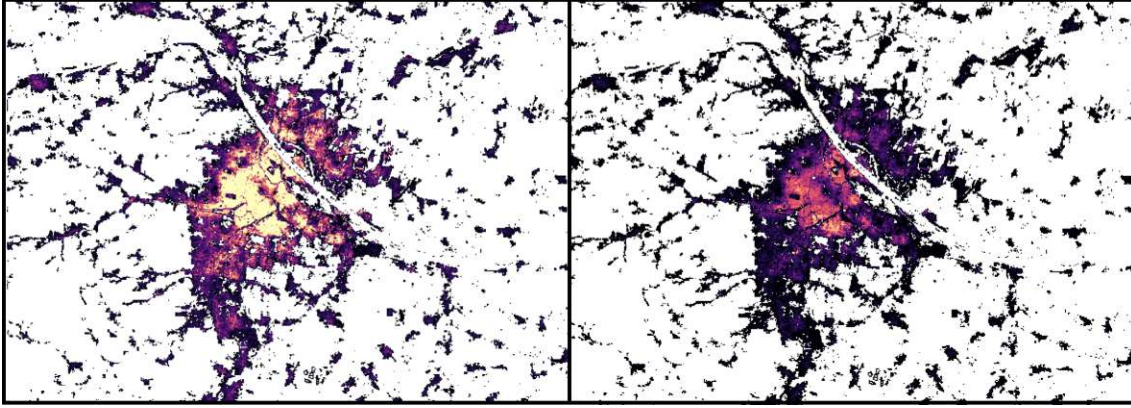


Figure 3.3: Total final energy demand of Austrian city of Vienna  $h^{fed}$  (left) and derived final energy demand covered by district heating  $h^{fed,dh}$  (right)

Finally, the final energy demand for space heating and hot water preparation covered by district heating ( $h_{i,j}^{fed,dh}$ ) was subtracted from the total final energy demand for space heating and hot water preparation ( $h_{i,j}^{fed}$ ), according to

$$h_{i,j}^{fed,rest} = h_{i,j}^{fed} - h_{i,j}^{fed,dh} \quad . \quad (3.4)$$

$h_{i,j}^{fed,rest}$  is further used for the calculation of the gas demand in each hectare.

### 3.3.2 Clustering Heat Demand Hectares

Another determinant for the existence of gas supply is the spatial accumulation of hectares with final energy demand. The clustering was performed by the python module DBSCAN from the SciKit-library [32]. The main idea behind the Density-Based Spatial Clustering of Applications with Noise (DBSCAN) module is that it assigns points belonging to a cluster if they are close to many points from that cluster. This allows the classification of distributed points, whether they are part of a cluster (core point, border point) or not (outliers). The clustering of the module is controlled by two key parameters: The first parameter EPS defines the distance that specifies the neighbourhood of a point. Two points are considered to be neighbours if the distance between them is less than or equal to EPS. The second parameter minPts defines the minimum number of data points to define a cluster. A point is defined as a core point, if it has at least minPts number of points (including the point itself) in its surrounding area with radius EPS. A border point is a point that is in the neighbourhood of a core point, but has less than minPts number of points within its surrounding area. An outlier is neither a core point nor is it in the neighbourhood of a core point. Figure 3.4 may explain these points better. The red points (A) are identified as core points because there are at least 4 points (minPts = 4) within their surrounding area with radius EPS, shown as the red circle. The yellow points (B, C) are defined as border points because they are reachable by core points but their neighbourhood consists of less than 4 points. The blue point (N) is neither a core point nor is it reachable from a core point.

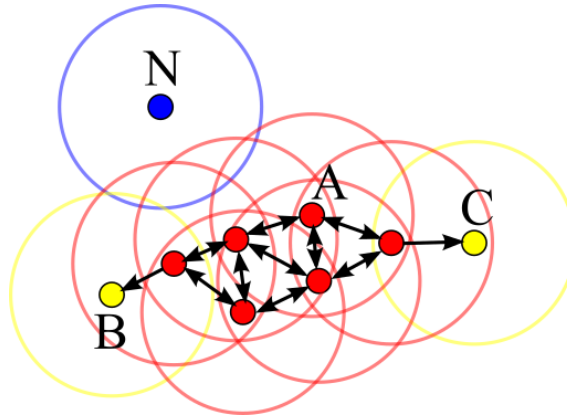


Figure 3.4: Illustration of parameters  $EPS$  and  $minPts$  in python module *DBSCAN* [33]

The same method is used to identify, whether hectares with a final energy demand are part of clusters that consists of close hectare elements with final energy demand. To apply the method, hectare elements with a final energy demand were converted into points that are located in the centre of the hectare element. The resulting map is similar to a scatter plot with a resolution of  $100\text{ m}$ , consisting of distributed points. In the next step, the map was processed with the *DBSCAN* module: Based on the two parameters  $EPS$  and  $minPts$ , a point (or associated hectare element with a final energy demand) is classified as a core point, as a border point or as an outlier. Assuming that gas supply infrastructure is only present in areas with a high density of final energy demand, it is considered unlikely that hectares that are associated with classified outliers will be supplied with natural gas. Therefore, each hectare element's final energy demand that is associated with a classified outlier, is set to  $0\text{ MWh}$  and thus is deleted from the map. Each hectare element's point that is identified as a core point or as a border point, is assigned to its surrounding cluster and the associated hectare element's final energy demand remains on the map. In the last step, each identified cluster's total final energy demand was calculated by summation of all hectare elements' final energy that were located within the respective cluster. If the sum exceeds a user-defined threshold  $h^{\text{cluster demand}}$ , the identified cluster remains, else the final energy demand of each hectare in the cluster is set to  $0\text{ MWh}$ . Figure 3.5 shows an example of clustered (hectare) elements. Each tile has a size of  $100\text{ per }100\text{ m}$  and demonstrates a hectare element. The coloured tiles indicate hectares with a final energy demand between  $0.1\text{ MWh}$  and  $1\text{ MWh}$ . All uncoloured hectares have no final energy demand. The colour of the respective hectare is scaled by the value of the final energy demand. The **X** in the hectares indicate the position of the points associated with the respective hectares.

In this example, the algorithm identifies one outlier (N) and two clusters (A and B) with  $EPS = 200\text{ m}$  and  $minPts = 4$ . A hectare is considered within the neighbourhood of another hectares, if its surrounding circle with radius of  $200\text{ m}$  touches the centre of neighbouring hectares. Hectares final energy demand that are identified as outliers are set to  $0\text{ MWh}$ . Depending on the set threshold for the total final energy demand per cluster, cluster A and B remain or not. If the value for  $h^{\text{cluster demand}}$  is set to  $2\text{ MWh}$ , hectare elements final energy demand of cluster A would be set to  $0$ , because the sum of all hectares final energy demand within this cluster ( $0.2 + 0.3 + 0.5 + 0.1 = 1.1\text{ MWh}$ ) is smaller than  $2\text{ MWh}$ . Cluster B would remain, because the sum of the hectares final energy demand ( $1 + 0.3 + 0.4 + 0.2 + 0.5 = 2.4\text{ MWh}$ ) is greater than  $2\text{ MWh}$ .

Figure 3.6 shows an example of clustered final energy demand for the Austrian city of

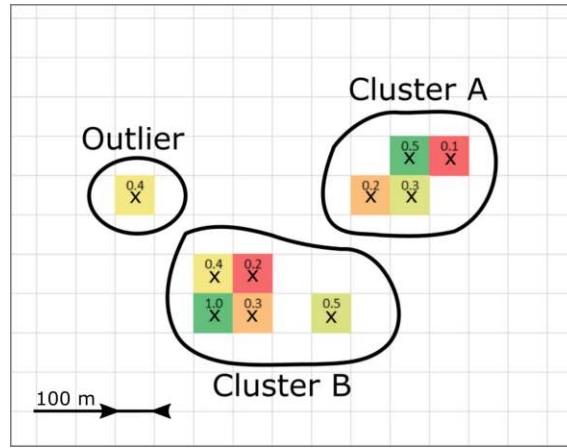


Figure 3.5: Illustration of clustering of hectare elements with dummy values for final energy demand in a 100 x 100 m raster

Vienna. The left panel of the Figure shows the reduced final energy demand from Equation 3.4 and the right panel shows the same city but with clustered hectare elements. The clustering in this example has been performed with  $EPS = 200\text{ m}$ ,  $minPts = 5$  and  $h_{cluster\ demand} = 12\text{ GWh}$ .

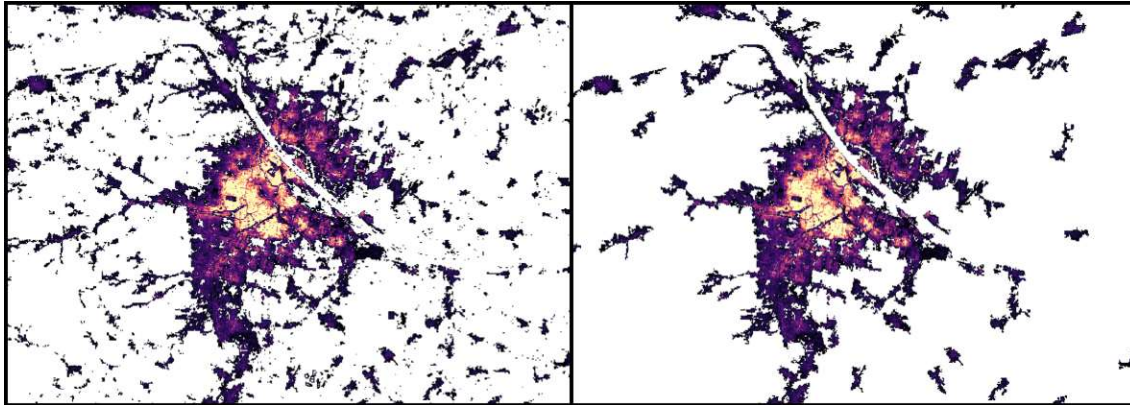


Figure 3.6: Unclustered final energy demand of Austrian city of Vienna  $h^{fed,rest}$  (left) and clustered final energy demand of same city  $h^{fed,clustered}$  (right)

The calculation of the potential gas share  $pot_{i,j}^{gas}$  is based on a similar equation as Equation 3.1, with  $h^{fed,clustered}$  and  $limit_{gas}$  instead of  $h^{fed,clustered}$  and  $limit_{dh}$ . The clustered final energy demand for space heating and hot water  $h_{i,j}^{fed,clustered}$  that exceed a user-defined threshold  $limit_{gas}$  are assumed to be fully supplied by gas. Below this threshold, gas supplies only a part, according to

$$pot_{i,j}^{gas} = \begin{cases} \frac{h_{i,j}^{fed,clustered}}{limit_{gas}}, & \text{for } h_{i,j}^{fed,clustered} \leq limit_{gas} \\ 1, & \text{for } h_{i,j}^{fed,clustered} > limit_{gas} \end{cases}, \quad (3.5)$$

where  $pot_{i,j}^{gas}$  is the potential share of gas in hectare  $(i, j)$  based on the clustered final energy demand for space heating and hot water preparation ( $h_{i,j}^{fed,clustered}$ ).

A further introduced parameter correlates the potential gas share of a hectare element to the distance to the closest European gas transmission line. Because gas is based on pipeline-based transport, the existence of a distribution network in a hectare is assumed to depend on the distance to next European transmission line. Therefore, the potential gas share  $\text{pot}_{i,j}^{gas}$  in hectare  $(i, j)$  is additionally weighted with a connection probability factor  $w_{i,j}^{con}$ . The weighted potential gas share  $\text{pot}_{i,j}^{gas,con}$  has full potential at hectares that consist of transmission lines and decrease linearly until a user-defined distance  $d^{eff}$ . The weighted potential gas share is defined according to

$$\text{pot}_{i,j}^{gas,con} = \text{pot}_{i,j}^{gas} \cdot w_{i,j}^{con} \quad . \quad (3.6)$$

### 3.3.3 Calculation of Connection Probability

Assuming hectares that are closer to the European transmission line are more likely to consist of a gas supplying infrastructure. Therefore the parameter  $w_{i,j}^{con}$  indicates the assumed probability of gas supply based on the distance to the next European transmission line in a hectare element. The parameter  $w_{i,j}^{con}$  is derived from the European Network of Transmission System Operators for Gas (ENTSO) Transmission Capacity Map 2019 [34], which is published annually in a ‘pdf’ format by ENTSOG, an association of the European transmission system operators. The capacity map consists of transmission pipelines, drilling platforms, Liquid Natural Gas (LNG) terminals and other assets of the European natural gas transmission network (Figure 3.7). SciGRID\_gas [29] converted this map into a geographically referenced object and published it in the GIS-vector format ‘geojson’ under an open-source licence, which made it accessible for spatial analyses. The conversion from the SciGrid\_gas map into a connection probability raster  $w_{i,j}^{con}$  is shown in Figure 3.8 for the example region of Vienna. In the upper left panel (#1) the blue lines indicates parts of the European transmission network from the SciGrid\_gas map. In a first step, this map is converted into a hectare raster. Hectare elements that are crossed by a transmission line are assigned the value 1, all other hectares are assigned the value 0. The right upper panel in Figure 3.8 (#2) shows the result of this step. In a second step, each hectare element with the value 0 is assigned the value  $d_{i,j}$  corresponding on the distance to the next transmission line. The further away a hectare element is from the next transmission line, the higher is its value. The lower left panel (#3) shows such a distance raster for example region of Vienna, shown as the blue-scaled shape. The higher the value of  $d_{i,j}$  in the respective hectare, the brighter is its colour.

Assuming that the probability of a gas supply decreases linearly with increasing distance to the next European transmission line, the connection probability raster  $w_{i,j}^{con}$  is defined, according to

$$w_{i,j}^{con} = \begin{cases} 1 - \frac{1}{d^{eff}} \cdot d_{i,j}, & \text{for } d_{i,j} \leq d^{eff} \\ 0, & \text{for } d_{i,j} > d^{eff} \end{cases} \quad . \quad (3.7)$$

$d^{eff}$  is a user-defined model input. The resulting map shows a linearly decreasing probability from the European transmission network to the user-defined distance  $d^{eff}$ . The connection probabilities of the hectares at transmission lines equal 1 and decrease to 0 of hectares at distances  $d^{eff}$ . Hectare elements that are further away than  $d^{eff}$  from the nearest transmission line have a connection probability of 0. The lower right panel (#4) in Figure 3.8 shows a connection probability raster for Vienna as a grey-scaled shape. For the sake of this example,  $d^{eff}$  was assumed to be 10 km to show the decreasing probability over Vienna. The black areas indicate hectare elements with a connection probability of 0. Generally, the chosen value for  $d^{eff}$  is higher, as it is very unrealistic that half of Vienna is disconnected from the gas distribution network.





Figure 3.7: A section of the ENTSOG Transmission Capacity Map 2019 [34]

### 3.3.4 Gas Demand of NUTS 3 Regions

To calculate the final energy demand covered by gas  $h_{i,j}^{fed,gas}$  for each hectare  $(i, j)$ , the clustered final energy demand  $h_{i,j}^{fed,clustered}$  from Section 3.3.2 is multiplied with the weighted potential gas share from Equation 3.6 and a discrepancy factor  $f^{dis,gas}$ , according to

$$h_{i,j}^{fed,gas} = h_{i,j}^{fed,clustered} \cdot pot_{i,j}^{gas,con} \cdot f^{dis,gas} \quad (3.8)$$

The factor  $f^{dis,gas}$  serves as a scaling factor, to meet the national share of gas  $x^{gas}$  in the supply mix for space heating and hot water preparation. It is calculated by

$$f^{dis,gas} = \frac{\sum_{i,j}^{region} h_{i,j}^{fed,clustered} \cdot x^{gas}}{\sum_{i,j}^{region} h_{i,j}^{fed,clustered} \cdot pot_{i,j}^{gas,con}} \quad (3.9)$$

The left panel of Figure 3.9 shows the clustered final energy demand  $h_{i,j}^{fed,clustered}$  of Vienna from Section 3.3.2 and the right panel the derived final energy demand covered by gas  $h_{i,j}^{fed,gas}$  calculated by Equation 3.8.

The total final energy demand in each NUTS 3 region  $E^{building,gas}$ , which is covered by

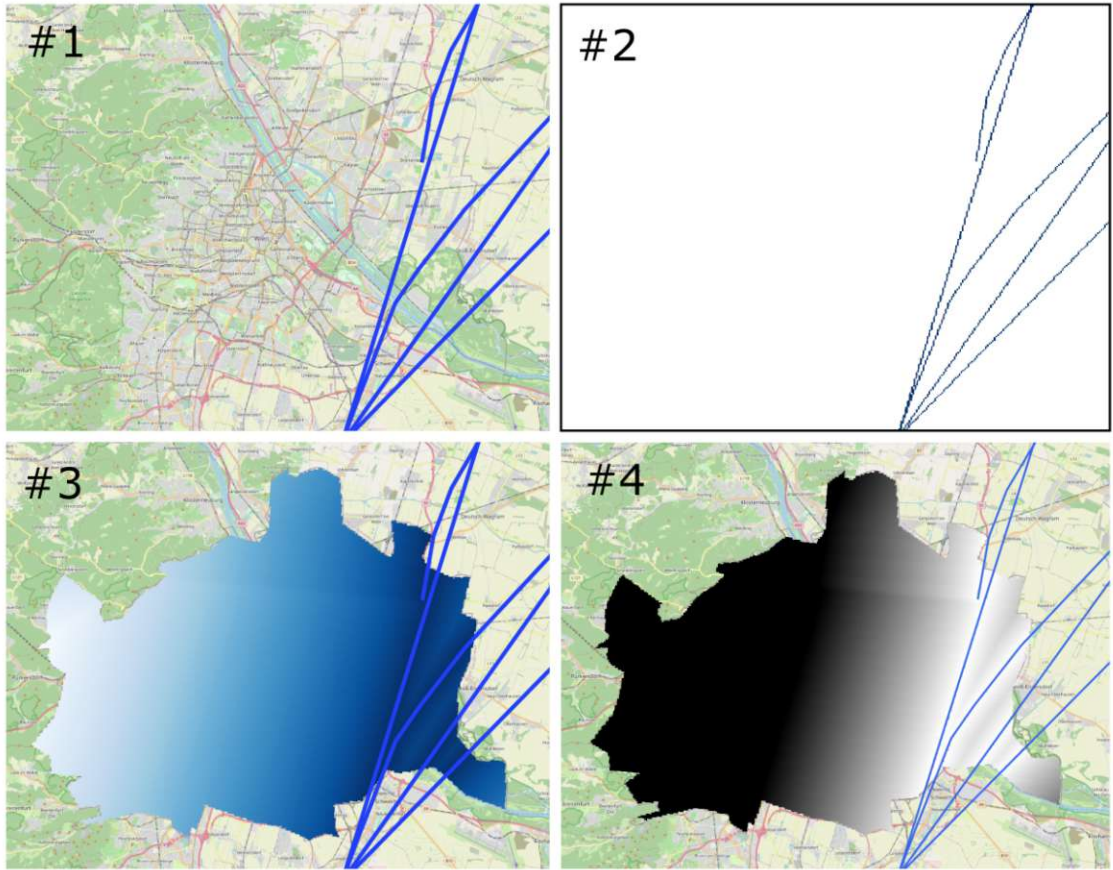


Figure 3.8: Workflow from the SciGrid\_gas map into a connection probability raster

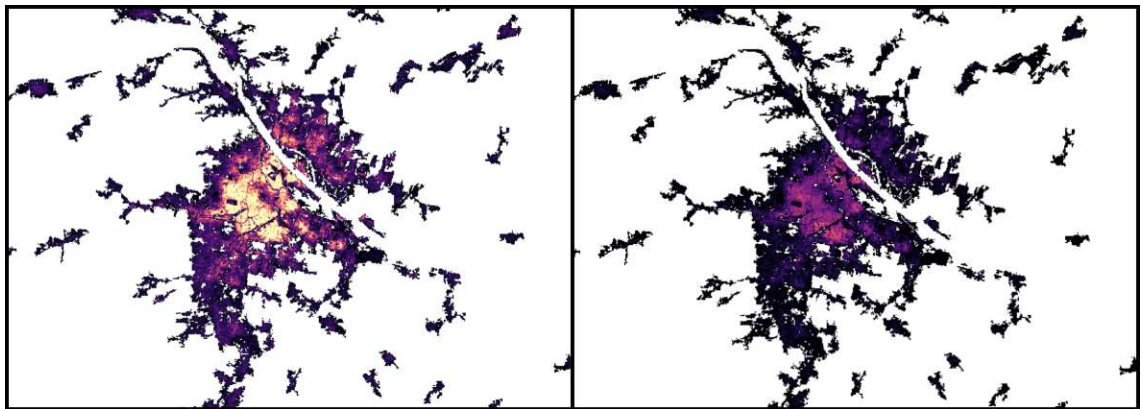


Figure 3.9: Clustered final energy demand  $h^{fed,clustered}$  of Vienna (left) and final energy demand of same city covered by gas  $h_{i,j}^{fed,gas}$  (right)

gas, is calculated by summing over all  $h_{i,j}^{fed,gas}$ , which are located in the respective region, according to

$$E^{building,gas} = \sum_{i,j}^{region} h_{i,j}^{fed,gas} \quad . \quad (3.10)$$

Figure 3.10 shows the summation border of the NUTS 3 regions where the orange line indicates the border of the NUTS 3 region from Equation 3.10. The coloured spots in Figure 3.10 indicate the hectare elements with a final energy demand for gas  $h_{i,j}^{fed,gas}$ . The labels within the regions are the registered NUTS 3 region names.

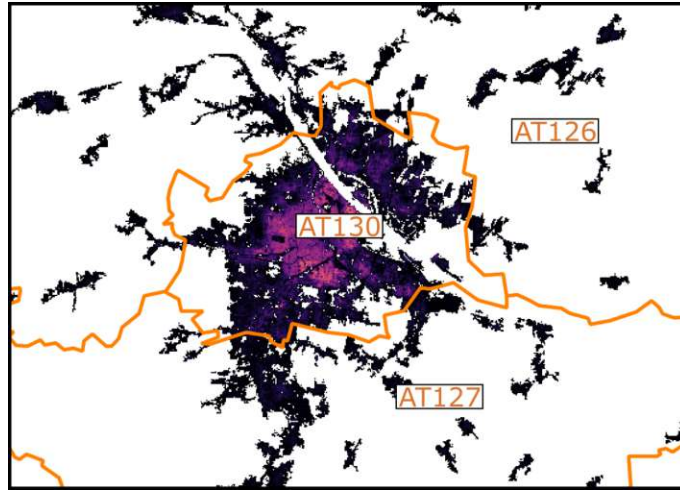


Figure 3.10: Yellow lines indicate the summation border of the NUTS3 region

### 3.4 Length Estimation of Gas Networks

Open-source information about the location of network assets does not exist on a regional level. Therefore the estimation of the gas network length per NUTS 3 region is based on a two-step approach: First, the gas network length is estimated based on the number of gas supplied buildings per hectare. Second, the total length of the gas network length per NUTS 3 region is calculated by summation of all resulting gas network lengths per hectare within the regions. The gas network length per hectare estimation is based on an empirical model from [27]. This approach estimates the minimum network length  $l_{i,j}^{buildings,gas}$  that is needed for connecting a set of gas supplied buildings  $n_{i,j}^{buildings,gas}$  in a hectare  $(i, j)$ , according to

$$l_{i,j}^{buildings,gas} = L^{chambers}(n_{i,j}^{buildings,gas}) \quad , \quad (3.11)$$

where  $l_{i,j}^{buildings,gas}$  defines the resulting (minimum) network length in the respective hectare element  $(i, j)$  and  $L^{chambers}$  defines the function from [27] that calculates the network length based on the number of gas supplied buildings in this hectare. The number of gas supplied buildings per hectare is calculated by first calculating the total number of buildings located in a hectare  $n_{i,j}^{buildings}$ , which is mainly derived from the OSM database. Second, multiplying the total number of buildings  $n_{i,j}^{buildings}$  with the potential gas share  $pot_{i,j}^{gas,con}$  from Equation 3.6. In summary, the overall workflow of network length estimation from the number of buildings calculation to the calculation of the total gas network length per NUTS 3 region is: First, downloading the building polygons from the OSM database and masking their centres as points. Then overlaying a hectare raster and counting the number of points for each hectare. Finally, based on the number of points per hectare estimating the minimum network length  $l_{i,j}^{buildings,gas}$  for any selected region. The following sections describe the workflow in detail.

### 3.4.1 Number of Gas supplied Buildings

Before calculating the minimum network length the number of gas supplied buildings on this hectare has to be determined. Geographical referenced positions and shapes of European buildings are available and freely accessible on the OSM database [35]. The OSM is created by volunteers and contains information about streets, buildings and other geographically referenced data all over the world. It has an *Open Data Commons Open Database Licence* [36], which makes the map and the underlying data free to use. To reduce the amount of data to download from the OSM database, filtered OSM data are used from the *www.geofabrik.de* database [37]). The building data is provided as polygons.

Figure 3.11 shows the workflow from the building polygons to the calculation of the number of buildings per hectare ( $n_{i,j}^{buildings}$ ). The single panels are created by QGIS [38], a free open-source-geographic-information software. The upper left panel in Figure 3.11 shows a district of Vienna from the OSM. In the first step, the underlying building polygons were downloaded from the *www.geofabrik.de* database, shown as the yellow polygons in the upper right panel of Figure 3.11. In the second step, the polygons were converted into yellow points (lower left panel in Figure 3.11). In the last step, the points are transferred on a hectare raster, the so-called *number-of-buildings-per-hectare* raster, which contains the number of buildings per hectare ( $n_{i,j}^{buildings}$ ), with the different shades of grey in the tiles indicating the numbers of buildings (lower right panel in Figure 3.11).

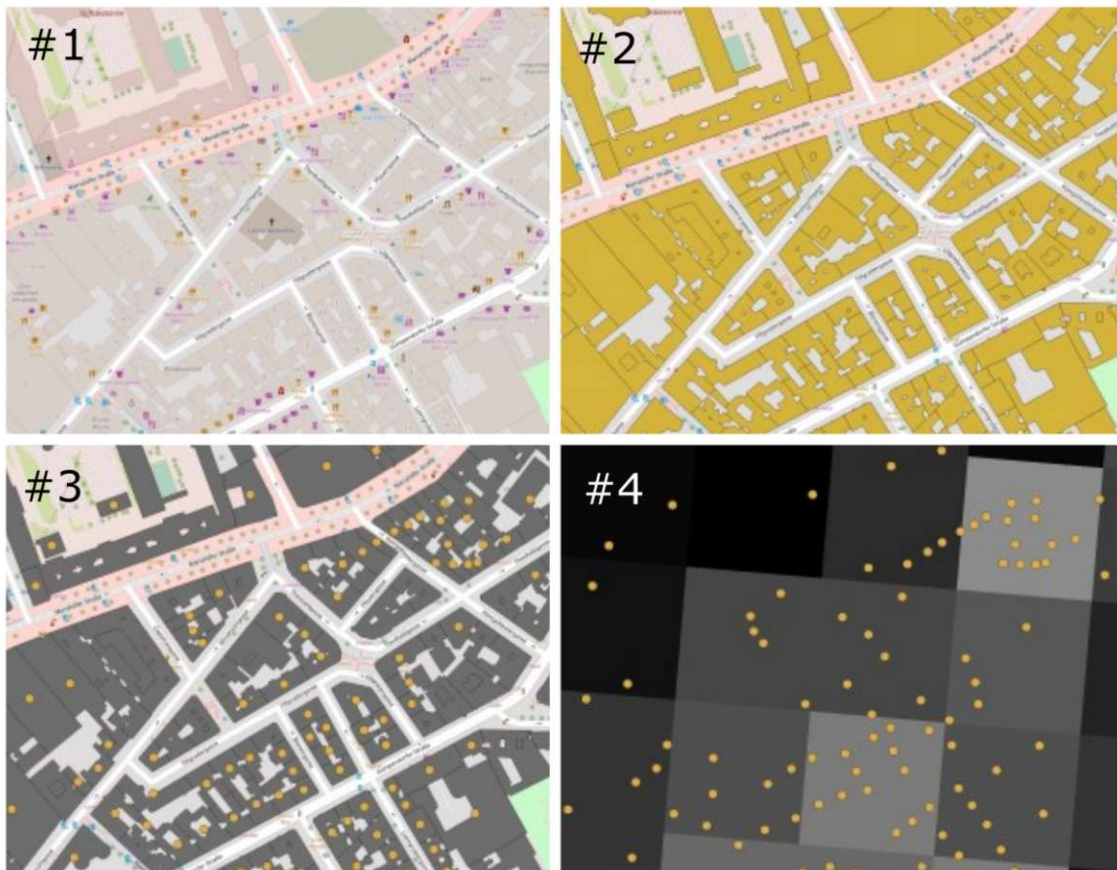


Figure 3.11: Workflow of generating the number-of-buildings-per-hectare raster

As an example, Figure 3.12 shows the *number-of-buildings-per-hectare* raster of the NUTS 3 region of Vienna as a grey scaled layer on top of the OSM layer of Vienna.

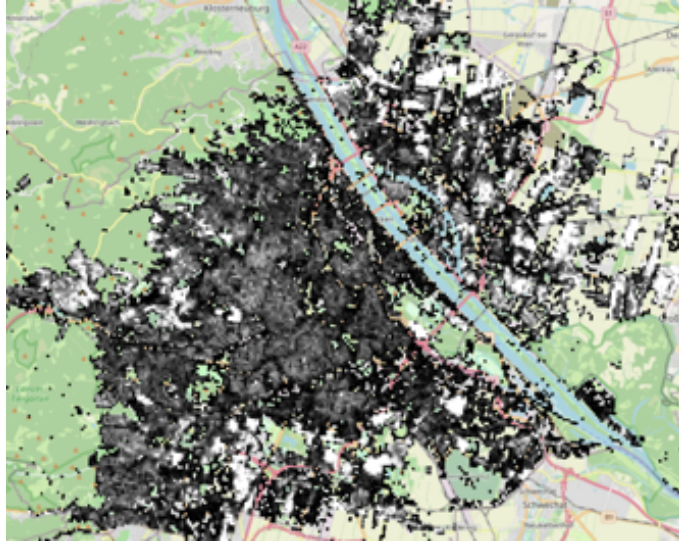


Figure 3.12: OSM section of Vienna, overlaid with number-of-buildings-per-hectare raster (grey-scaled raster)

The OSM database is a community-supported project. The coverage of building data depends highly on the activity of the local OSM community. Therefore data coverage is unevenly distributed over Europe. To get a more complete data set, the calculated map was improved by the building footprint density map from the hotmaps project [28]. This map contains the building footprint  $bf_{i,j}$  per hectare ( $i, j$ ) for the EU-27 + Switzerland, Norway, Iceland and UK. The data set is based on the building data of the OSM database [35] from 2015 and on the European Settlement Map [39]. The European Settlement Map contains information about the human settlement on a  $10 \times 10$  m level from satellite imagery. To get a more complete *number-of-buildings-per-hectare* raster, in a first step the average building footprint per building  $a_{i,j}$  in a hectare was calculated by dividing the hotmaps' building footprint  $bf_{i,j}$  with the calculated number of buildings  $n_{i,j}^{buildings}$ , according to

$$a_{i,j} = \frac{bf_{i,j}}{n_{i,j}^{buildings}} \quad . \quad (3.12)$$

In the next step, hectares where  $a_{i,j}$  exceeds a user-defined threshold ( $a_{max}$ ) a newly calculated number of buildings per hectare ( $n_{i,j}^{buildings,new}$ ) replaces the current  $n_{i,j}^{buildings}$  in the respective hectare by dividing  $bf_{i,j}$  with a user-defined estimation of the average building footprint per building ( $bf_{building}$ ), according to

$$n_{i,j}^{buildings,new} = \begin{cases} \frac{bf_{i,j}}{bf_{building}}, & \text{for } a_{i,j} \geq a_{max} \\ n_{i,j}^{buildings}, & \text{for } a_{i,j} < a_{max} \end{cases} \quad . \quad (3.13)$$

In case a hectare contains a few large buildings, indicated by a large building footprint on the building footprint density map, but the calculated  $n_{i,j}^{buildings}$  contains no building, the newly calculated number of buildings  $n_{i,j}^{buildings,new}$  within this hectare is overestimated. This fact should be kept in mind when assessing the results.

Assuming that the existence of a gas distribution network in a hectare depends on the number of buildings. Therefore, in hectares where the value for  $n_{i,j}^{buildings,new}$  is smaller than a user-defined value ( $n_{i,j}^{buildings,min}$ ), the value for  $n_{i,j}^{buildings,new}$  is set to 0 buildings,

according to

$$n_{i,j}^{buildings,new} = \begin{cases} n_{i,j}^{buildings,new}, & \text{for } n_{i,j}^{buildings,new} \geq n^{buildings,min} \\ 0, & \text{for } n_{i,j}^{buildings,new} < n^{buildings,min} \end{cases} \quad (3.14)$$

The number of gas supplied buildings per hectare was calculated by multiplying the number of buildings per hectare ( $n_{i,j}^{buildings,new}$ ) with the potential gas share  $\text{pot}_{i,j}^{gas,con}$  from Equation 3.6 and a discrepancy factor  $f^{dis,n}$ , according to

$$n_{i,j}^{buildings,gas} = n_{i,j}^{buildings,new} \cdot \text{pot}_{i,j}^{gas,con} \cdot f^{dis,n} \quad (3.15)$$

Assuming that not all buildings in an identified gas supplied area are connected to the gas distribution network, the factor  $f^{dis,n}$  serves as a scaling factor, to meet the national share of gas supplied buildings in identified gas supplied areas, according to

$$f^{dis,n} = \frac{\sum_{i,j} n_{i,j}^{buildings,new} \cdot \text{pot}_{i,j}^{gas,con} \cdot x^{gas,n}}{\sum_{i,j} n_{i,j}^{buildings,new} \cdot \text{pot}_{i,j}^{gas,con}} \quad (3.16)$$

The variable  $x^{gas,n}$  thus indicates the national share of buildings connected to the gas network in areas where a gas distribution (potentially) exists. For example, if 100 buildings are located in an area, where a gas distribution network potentially exists and 20 buildings are connected to this distribution grid, the share  $x^{gas,n}$  is 20 %.

### 3.4.2 Empirical Model Fit

Planning a pipe network is a complex process. It requires a detailed look at local conditions such as roads, geographic formations, underground installations, buildings, etc. Since most of these conditions are difficult to account for in each region for a European wide approach, an overall statistical approach is needed to estimate the network length. Calculating the shortest connection between a set of buildings could be a solution for estimating the minimum network length. This is a well-known problem in graph theory, called the Minimum-Spanning-Tree Problem (MST). It can be performed for a set of nodes by the Kruskal algorithm [40] where the nodes are the centre positions of the buildings. This algorithm is quite intense when applied on a national scale. In [27] the minimum connection for a set of buildings for a sample of hectares was calculated by using MST. They observed, that the gas supplied buildings per hectare are the main determinant of minimum pipe length and could derive an empirical model to calculate the minimum network length  $l_{i,j}^{building,gas}$  of hectare ( $i, j$ ) based on the number of gas supplied buildings in this hectare ( $n_{i,j}^{buildings,gas}$ ), according to

$$l_{i,j}^{building,gas} = 130.6 \cdot \ln(n_{i,j}^{buildings,gas}) - 84.5 \quad (3.17)$$

Figure 3.13 shows the logarithmic relation between the number of gas supplied buildings per hectare  $n_{i,j}^{buildings,gas}$  and pipe length (= minimum network length  $l_{i,j}^{building,gas}$ ) according to Equation 3.17. The coefficients of the model were found by [27] using a linear regression, with a determination coefficient of  $R^2 = 0.984$ .

Equation 3.17 was used to estimate the minimum gas distribution network length in a hectare to supply a set of buildings.

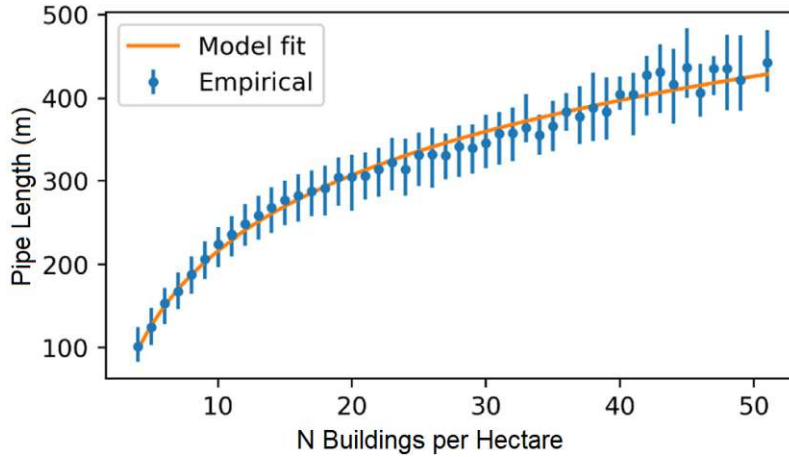


Figure 3.13: Exponential model fit based on the minimum pipe length as a function of numbers of buildings per hectare [27]

### 3.4.3 Minimum Gas Distribution Length of NUTS 3 Regions

To calculate the minimum network length per hectare for a set of gas supplied buildings Equation 3.17 is applied to  $n_{i,j}^{buildings,gas}$ . To obtain the total gas network length for gas supplied buildings in a selected NUTS 3 region, all hectare elements' network lengths that are located in the region are summed up, according to

$$l^{building,gas,total} = \sum_{i,j}^{region} l_{i,j}^{buildings,gas} \quad , \quad (3.18)$$

where  $l^{building,gas,total}$  is the total minimum network length to supply all gas supplied buildings in the selected NUTS 3 region.

## 3.5 Gas Demand and Network Length of the Power generating Sector

As already mentioned, the model in the current version does not take into account the gas demand and the grid length of gas-fired power plants. Nevertheless, a module has been developed that has already been implemented and can be further developed in the future. Therefore, the module will be briefly presented here. The input data for this module is extracted from JRC Open Power Plants Database (JRC-DB) [41], which is an incomplete collection of European power plants and their indicators like peak power, efficiency, geographic location, etc.

Power stations are generally directly connected to the European transmission network [42]. Therefore all gas power stations in a NUTS 3 region are connected first to a virtual point in the regional centre. Then the centre is connected to the next European transmission line. The total length of the supply pipe is assumed to be approximately the sum of distances from all power stations to the centre of the region  $l^{power,gas}$  plus the distance from the regional centre to the next European transmission line  $l^{ETN}$ ,

$$l^{power,gas,total} = \sum_i^{region} l_i^{power,gas} + l^{ETN} \quad . \quad (3.19)$$

The yellow points in Figure 3.14 show the position of gas power plants in the NUTS 3 region of Vienna (pink shape) and the green point shows the centre of the region. The black lines ( $l_1, l_2, l_3, l_4$ ) indicate the distances between the power plants and the centre of the region.

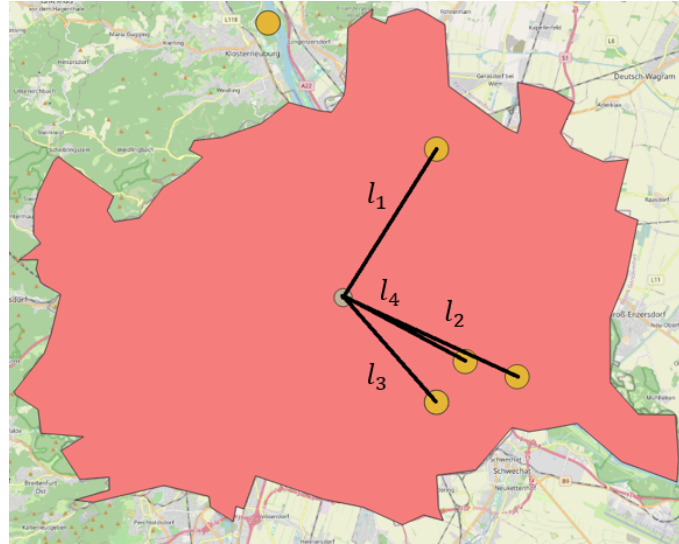


Figure 3.14: Total length calculation of the transmission network

To calculate the gas demand of gas power plants, first, all power plants that are located in the region boundary and are operated by gas were extracted from JRC-DB. Then the gas consumption was calculated by multiplying the unit capacity  $p^{peak}$  with an estimation of the full load hours  $h^{flh}$  and divided by the efficiency of the generation unit  $\eta^{pp}$ . The calculation follows

$$E^{gas,pp} = \frac{p^{peak} \cdot h^{flh}}{\eta^{pp}} \quad . \quad (3.20)$$

### 3.6 Network Cost Estimation

The *network-cost-calculation* (CM #4) module in the OGIS model calculates the NPV of gas distribution grids. The net present value is the sum of present values of all revenues and expenditures within the service life of the gas network. The referenced date, to which the NPV is calculated, is the defined base year. Every cash flow (= costs or revenues) before the referenced date is compounded and every cash flow after the referenced date is discounted to the base year. The user-defined calculation interest rate  $i$  defines the compound- or discount-rate ( $q = 1 + i$ ). As discussed in Section 2.5.1, the profitability of a network is given, when the absolute value of the NPV is greater or equal to zero. The absolute NPV is calculated according to

$$NPV_{\text{base year}} = R_{his} - C_{his} - I_{his} + \sum_{t=0}^n (R_t - C_t) \left(\frac{1}{q}\right)^t + RV \quad , \quad (3.21)$$

$$n = \text{target year} - \text{base year} \quad , \quad (3.22)$$



where  $NPV_{\text{base year}}$  describes the net present value of the network referenced to the base year.  $R_{his}$  is the sum of all revenues gained in the past,  $C_{his}$  is the sum of all expenditures spent in the past,  $I_{his}$  is the investment spent in the past to build the network and  $RV$  is the residual value of network assets after the target year. The sum in Equation 3.21 includes all revenues  $R_t$  and expenditures  $C_t$  that occur between the base year and the target year.

### 3.6.1 Development of Gas Demand and Network Length

The variables in the NPV calculation are mainly based on the gas demand and the network length of the respective years. However, both values are only calculated for the base year and the target year. For the NPV calculation, both values are needed in each year from the beginning of the network service life, which is assumed to be before the base year until the end of the network service life, which is assumed to be after the target year. For the years between the base year and target year, the values are linearly interpolated between both years. The values for both parameters before the base year and after the target year are assumed to be the values in the respective year. Figure 3.15 shows the assumed development of both values, whereas the development of only one parameter is shown, but it is the same for both. The example network in Figure 3.15 is constructed in 2010 and decommissioned in 2065. The base year is 2020 and the target year is 2050. The NPV is referenced to the base year 2020.

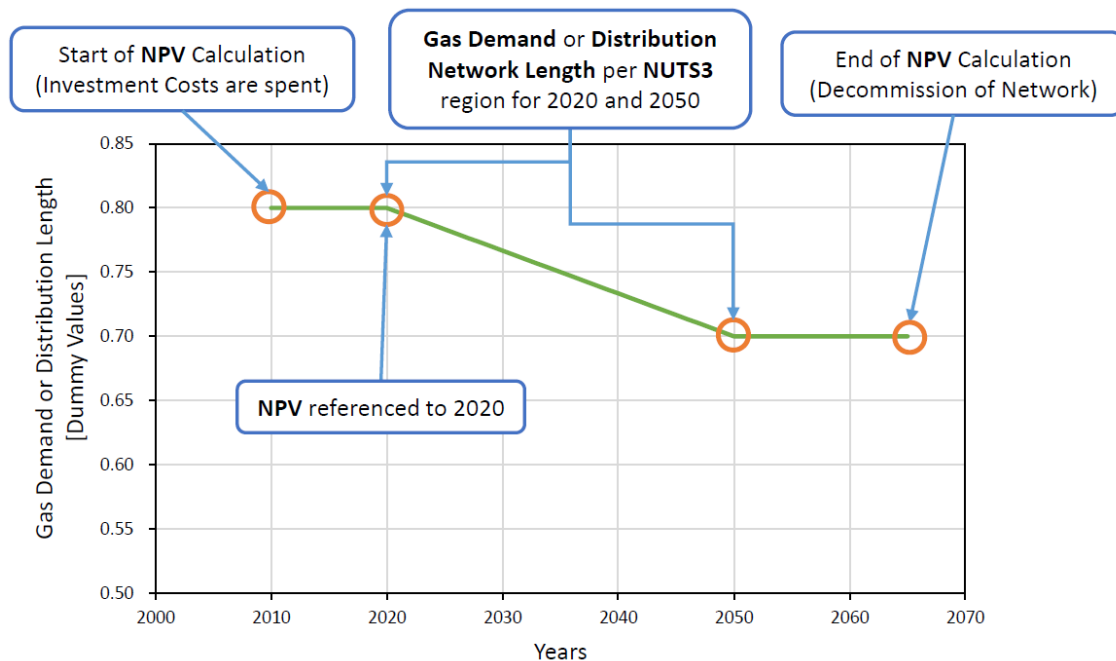


Figure 3.15: Assumed development of gas demand and distribution network length over the service life of a network

### 3.6.2 Calculation of NPV Parameters

Assuming that all gas network revenues come from grid charges, the historical revenue  $R_{his}$  calculation follows the summation of all grid charges before the base year. Historical revenues are modelled based on the final energy demand for gas  $E_{\text{base year}}^{\text{buildings,gas}}$  in the years before the base year and are described mathematically as

$$R_{his} = \sum_{t=0}^{\text{network age}} E_{\text{base year}}^{\text{buildings,gas}} \cdot c_{gc} \cdot (1 - r_{gc})^t \cdot q^t, \quad (3.23)$$

$$\text{network age} = \text{base year} - \text{construction year}, \quad (3.24)$$

where  $c_{gc}$  describes the grid charges defined in costs per unit energy,  $q$  compounds the respective revenue to the base year and  $r_{gc}$  defines the rate, by which the grid charge increases or decreases over the years. The network age, which is a user-defined input parameter, sets the average asset age of the gas network in the base year (Equation 3.24).

Costs for operating a network are referred to as operational expenditures (OPEX) and are constant costs for functioning business operations. The OPEX include costs for raw materials, supplies, personal costs, etc. and are modelled based on the network length and the final energy demand for gas [23]. To calculate the costs that are spent before the base year ( $C_{his}$ ), the values for both parameters in each year before the base year are set to the values in the base year (Figure 3.15), according to

$$\begin{aligned} C_{his} &= \sum_{t=0}^{\text{network age}} (\text{OPEX}_{\text{base year}}) \cdot (1 - r_c)^t \cdot q^t \\ &= \sum_{t=0}^{\text{network age}} (c_1 \cdot l_{\text{base year}}^{\text{buildings,gas}} + c_2 \cdot E_{\text{base year}}^{\text{buildings,gas}}) \cdot (1 - r_c)^t \cdot q^t. \end{aligned} \quad (3.25)$$

where  $c_1$  and  $c_2$  are user-defined cost parameters.  $c_1$  describes the length specific operational costs, which scales with network length and  $c_2$  aggregates costs caused by upstream grid charges, concession fees and loss costs. Parameter  $c_2$  scales with the amount of gas flowing through the network. The final energy demand for gas  $E_{\text{base year}}^{\text{buildings,gas}}$  and the total length of the network  $l_{\text{base year}}^{\text{buildings,gas}}$  for each year before the base year are set to the values in the base year.  $r_c$  is a user-defined rate, by which the operational expenditures change over the years.  $q$  compounds the costs to the base year.

The historical investments  $I_{his}$  in Equation 3.21 define the costs for constructing the network. Normally it takes several years to build a gas network and investment costs are distributed over these years. For simplicity, construction costs for distribution networks are referred to a user-defined year. The investment costs are calculated by multiplying the total length of the network  $l_{\text{base year}}^{\text{buildings,gas}}$  in the base year with costs per length  $c_p$ . These costs summarise all investment expenditures for pipes, apparatuses, buildings, etc. Historical investment costs are defined as

$$I_{his} = l_{\text{base year}}^{\text{buildings,gas}} \cdot c_p \cdot (1 - r_p)^t \cdot q^{\text{network age}}, \quad (3.26)$$

where the factor  $q$  compounds the investment cost to the base year.  $r_p$  defines the rate, by which the investment cost decrease or increase over the years.

During its service time, a yearly cash flow of expenditures and revenues secure the functionality of the gas network, which is taken into account in the sum in Equation 3.21. The sum consists of all revenues  $R_t$  and expenditures  $C_t$  which occur between the base year

( $t = 0$ ) and the target year ( $t = n$ ). The discounting factor ( $1/q$ ) discounts the yearly cash flow in year  $t$  to the base year. The calculation of the revenues and expenditures over the years depends on the network length and the final energy demand for gas in the respective year. The model calculates the network length and final energy demand for gas in the base year and the target year. The values for both parameters for the years in between are linearly interpolated (Figure 3.15).

Revenues of gas infrastructure come from grid charges which the network users pay. Like the historical revenues in Equation 3.23, the revenues are calculated by multiplying the final energy demand for gas  $E_t^{buildings,gas}$  in year  $t$  with the user-defined grid charge  $c_{gc}$ , according to

$$R_t = E_t^{buildings,gas} \cdot c_{gc} \cdot (1 + r_{gc})^t \quad . \quad (3.27)$$

The user-defined factor  $r_{gc}$  describes how the grid charge change over the years. Expenditures of a gas network consist of operational expenditures  $OPEX_t$ , costs for grid expansion  $I_{exp}$  and maintenance costs  $I_{main}$  according to

$$C_t = OPEX_t + I_{exp,t} + I_{main,t} \cdot irf_t \quad . \quad (3.28)$$

The operational expenditures  $OPEX_t$  in year  $t$  after the base year summarises all costs for operating the asset. Similar to the  $OPEX_{base\ year}$  in Equation 3.25 they scale with network length and final energy demand for gas in the current year according to

$$OPEX_t = (c_1 \cdot l_t^{buildings,gas} + c_2 \cdot E_t^{buildings,gas}) \cdot (1 + r_c)^t \quad . \quad (3.29)$$

The cost parameters  $c_1$  and  $c_2$ , the rate  $r_c$  and the factor  $q$  are equal to the values in Equation 3.25.  $I_{main,t}$  is defined as the amount of investment, which has to be made, to keep the network up to date and the average asset age at a constant level. It is equal to the yearly depreciation cost  $I_{depreciation,t}$ , based on the cost for investment  $I_t$  for the network length  $l_t$  in year  $t$ . The depreciation is defined as the investment costs divided by the service time of investment. Therefore the maintenance cost is defined according to

$$I_{main,t} = I_{depreciation,t} = \frac{I_t}{st} = c_p \cdot l_t(1 + r_p) \cdot \frac{1}{st} \quad , \quad (3.30)$$

where  $c_p$  describes the construction costs per network length,  $l_t$  the network length in year  $t$ ,  $r_p$  the rate at which the investment costs per network length increase or decrease over the years and  $st$  the service time of the network.

The yearly investment cost for network expansion  $I_{exp,t}$  is 0, when the length of the grid shrinks and greater than 0, when the network expands, according to

$$I_{exp,t} = \begin{cases} I_t - I_{t-1}, & \text{for } l_t^{buildings,gas} \geq l_{t-1} \\ 0, & \text{for } l_t^{buildings,gas} < l_{t-1} \end{cases} \quad . \quad (3.31)$$

The investment-reduction-factor  $irf_t$  in Equation 3.28 depends on the investment strategy of the network operator. It reduces or increases the expenses for maintaining the grid. If  $irf_t = 1$ , the state of the network does not change over the years, pipes get refurbished or constructed at the same rate, as old pipes get decommissioned. The quality of the network assets stays the same and the average asset age does not change. If  $irf_t < 1$  the average asset age gets older over time, refurbishment or construction actions happen at a lower rate, as old pipes get decommissioned. The average asset age is described by the Mean Rest Booking Value Factor (MRBVF) [23]. The MRBVF is 0 when the network is at the end of its service time and 1 when the network is newly constructed. Its value depends

on the current capital stock  $CS_t$  and the investment cost  $I_t$ . Its value must be calculated iterative according to

$$\begin{aligned} MRBVF_0 &= 1 - \frac{\text{network age}}{st} , \\ MRBVF_t &= \frac{CS_t}{I_t} . \end{aligned} \quad (3.32)$$

The initial value for the  $MRBVF_0$  depends on the user-defined average network age in the base year  $t = 0$  and the assumed service time of the network  $st$ . The  $MRBVF_t$  of following years is the ratio of the current capital stock  $CS_t$  and the current investment costs  $I_t$  in  $t$  years after the base year. The capital stock is per definition the economic capital of the network operator and summarises the actual economic value of the distribution network. It is the sum of all investments, which are made in the previous year, minus the depreciation costs. In case of shrinking network length due to the disconnection of customers, the network operators face physical capital (e.g. in form of pipes), which cannot be monetised by selling. Therefore these costs are seen as sunk costs and decrease the value of the capital stock, according to

$$\begin{aligned} CS_0 &= I_0 \cdot MRBVF_0 , \\ CS_t &= (CS_{t-1} + I_{exp,t-1} + I_{main,t-1}) - \frac{I_t}{st} - \begin{cases} I_{t-1} - I_t, & \text{for } l_{t-1} \geq l_t^{buildings,gas} \\ 0, & \text{for } l_{t-1} < l_t^{buildings,gas} \end{cases} . \end{aligned} \quad (3.33)$$

The capital stocks' initial value  $CS_0$  is the investment cost in the base year  $I_0$  multiplied by the mean rest booking value factor in the same year. The value for the capital stock is iteratively calculated for every following year after the base year.

For the calculation of the NPV, expenditures and revenues until the target year are considered. However, in the target year, the distribution network still has an economic value. This value is called residual value  $RV$  and is added to the NPV (Equation 3.21). The residual value of a network is defined as the sum of all revenues minus the sum of all operational costs that are made after the target year until the networks  $MRBVF$  reaches 0 in case no maintenance actions are performed after the target year. The gas demand and length of the network in all years after the target year are defined as equal to the gas demand and network length in the target year (Figure 3.15). The investment-reduction factor  $irf_t$  is set to 0 after the target year, which will decrease the  $MRBVF$  at a constant rate. The calculation of the residual value is defined as

$$RV = \sum_{t=n+1}^d (R_{\text{target year}} - OPEX_{\text{target year}}) \cdot 1/q^t . \quad (3.34)$$

where  $d$  is the number of years after the base year until the assumed network decommission.

## 3.7 Scenario Definition

### 3.7.1 Scenario Definition for Demand Projection

Two scenarios were chosen to calculate the NPV of the distribution grid in each NUTS 3 region in all EU-27 countries. The selected scenarios define the projection of the final energy demand for space heating and hot water preparation in the demand-projection tool (Section 3.2). The scenario files for the demand-projection tool were generated by the Invert/EE-Lab module [31] under the assumption of a carbon-neutral energy system

in 2050. The main input parameters for the scenario development under the Invert/EE-Lab module were derived from the PRIMES reference scenario. The PRIMES reference scenario 2020 (E3 Modelling 2020), provided by the EU Commission, determined parameters like macro-drivers, future development of energy prices and possible levels of energy services [43]. Other parameters like the carbon price for the Invert/EE-Lab were derived from the Impact Assessment of the Climate-Target Plan [44].

Two different assumptions on the share for gas for heating and hot water preparation distinguished the two input scenarios for the demand projection tool. The first scenario (Gas60) defines a 60 % gas share and the other scenario (Gas20) defines a 20 % gas share of total heated gross floor area in 2050 in the EU-27. Gas60 was developed, to simulate a scenario, in which gas still plays an important role in space heating and hot water preparation and Gas20 was developed to simulate a gas phase-out for space heating and hot water preparation after 2050. All other parameters like renovation-, construction- and demolition-rate, the national share of technologies final energy demand for space heating and hot water preparation ( $x^{gas}$ ,  $x^{dh}$ ), etc. were optimised under the predefined assumptions in the Invert/EE-Lab module in an ongoing research project [2]. The evaluated period was set from 2020 to 2050, where 2020 is the base year and 2050 is the target year. Both scenarios share the same assumptions in the base year and differ in the target year in the share of gas heated gross floor area.

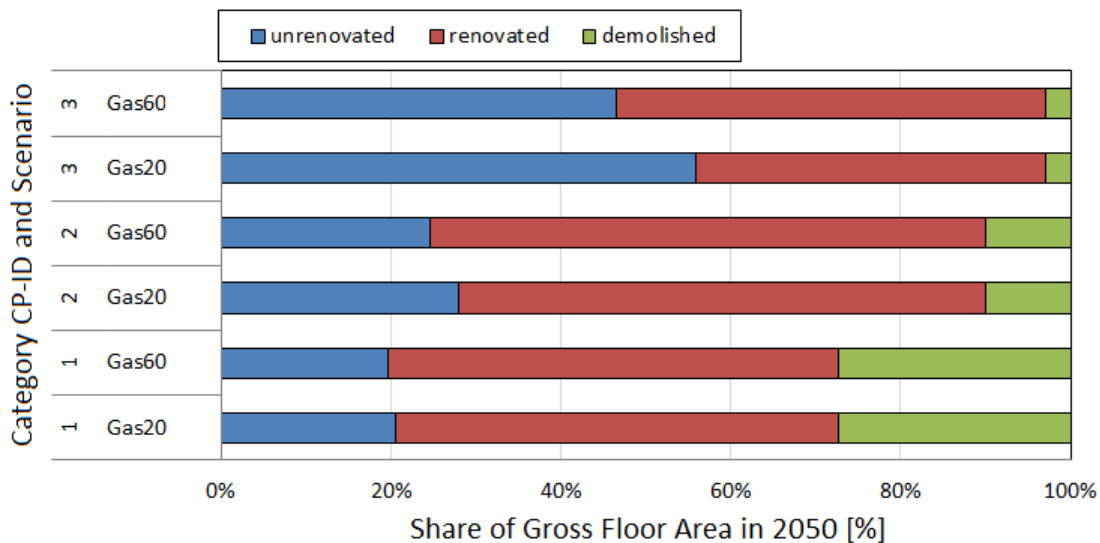


Figure 3.16: Share of unrenovated, renovated and demolished gross floor area from 2020 to 2050 per scenario and construction period

Figure 3.16 shows the change of gross floor area from 2020 to 2050 under the optimised renovation and demolition rates for each scenario and each construction period in EU-27 countries. The construction periods are identified by a Construction Period Identification Number (CP-ID), where CP-ID 1 are all buildings built before 1975, CP-ID 2 are buildings built between 1975 and 1980, CP-ID 3 are all buildings built between 1980 and 2000 and CP-ID 4 are all newly constructed buildings after 2000.

Due to the share of renovated gross floor area, the Figure shows more ambitious renovation rates in the Gas60 scenario than in the Gas20 scenario across all construction periods. Demolition actions happen at the same rate in both scenarios.

Figure 3.17 shows the decrease of the final energy demand across all construction periods

### 3. MATERIAL AND METHODS

from 2020 to 2050 in the EU-27 countries. The green boxes show the final energy demand for space heating in 2020. The yellow boxes show the same for the Gas20 and the purple boxes for the Gas60 scenario in 2050. The final energy demand in the Gas20 scenario is slightly lower than in the other scenario across all construction periods.

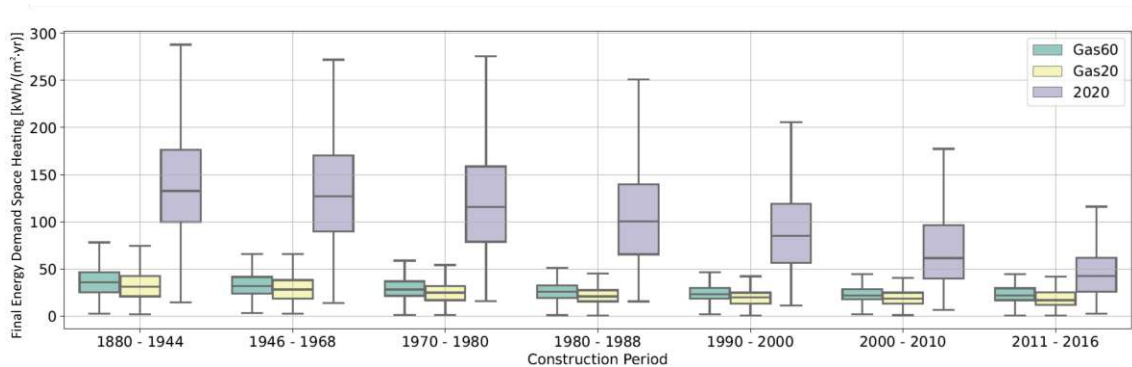


Figure 3.17: Final energy demand for space heating in year, scenario and construction period.

Figure 3.18 shows the share of gas technologies for space heating and hot water preparation in the final energy demand in 2020 and in 2050 in each scenario. Based on the share gas share of 2020, 11 out of 26 countries in the Gas60 scenario and 3 out of 26 countries in the Gas20 scenario show an increase of gas demand share in the Gas20 scenario. All other countries indicate a decrease of gas demand share to total supply mix in space heating and hot water preparation in 2050 in both scenarios.

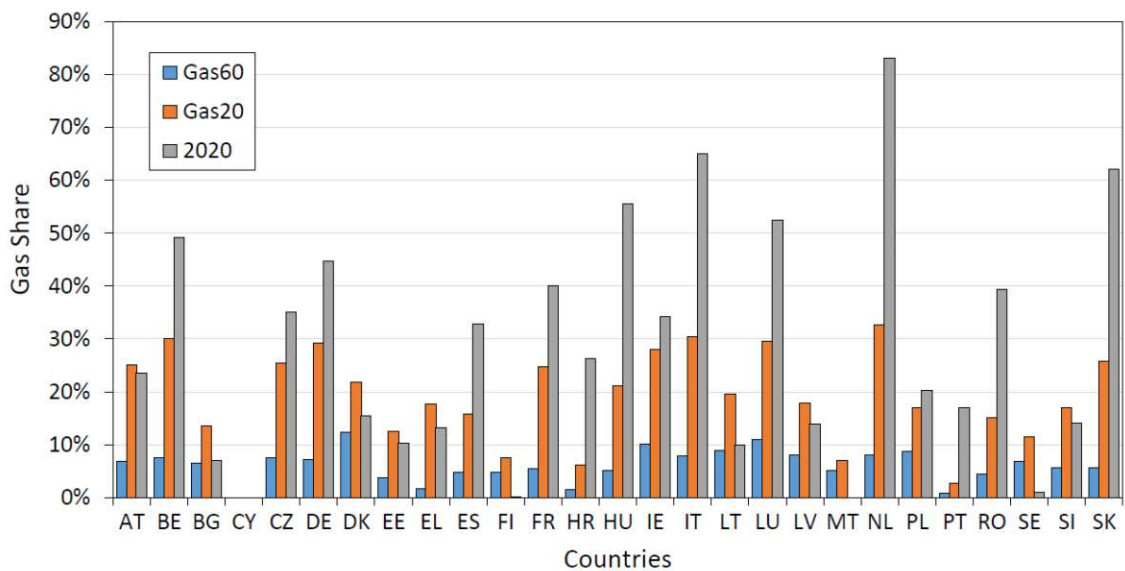


Figure 3.18: National share of gas in the supply mix for space heating and hot water preparation for each country in EU-27

With all these parameters from the Invert/EE-Lab module, the demand-projection tool calculated the heat demand density map for 2050 for both scenarios. The calculated map served as an input for the demand and network length calculation for selected NUTS 3 regions. The costs for gas distribution were calculated under the assumptions of the network strategy of network operators.

### 3.7.2 Scenario Definition for Network Strategy of Network Operators

The NPV was calculated to assess the economic profitability of gas networks as described in Section 3.6. The calculation of the network costs depends on several user-defined parameters, which determine the network strategy (e.g. rate of refurbishment-, or construction actions within the network). With the following assumptions, I tried to define a realistic economic behaviour of the network operator within the defined scenario.

The calculation of the NPV starts in the base year. Part of Equation 3.21 considers historical expenditures and revenues, which are counted from a user-defined year. The service time  $st$  of the network is set to 30 years, as it seems like a standard network lifetime before all-encompassing renovation activities must be made. The  $MRBVF_0$  in Equation 3.32 is 0.67, where the network consists of more assets younger than half of the service time.

The investment in network maintenance ( $I_{main,t}$ ) is considered to keep the asset quality at the same level until 2035 (constant  $MRBVF_t$  with  $t$  from 2020 – 2035). The investment reduction factor  $irf_t$  is set to 1. From 2035, network operators are assumed to reevaluate their economic network strategy. In the Gas60 scenario, the network operator reduces the yearly investment in maintenance, so that the average age of the network will be half of its service time in 2060 ( $MRBVF_{2060} = 0.5$ ). This indicates a network, which will be operated after 2060. In the Gas20 scenario, the network operator reduces the yearly investment in maintenance, so that the average age of the network assets are old as three-quarters of its service time in 2060 ( $MRBVF_{2060} = 0.25$ ). This indicates a gas phase-out situation, where the network is going to be decommissioned soon after 2060.



Die approbierte gedruckte Originalversion dieser Diplomarbeit ist an der TU Wien Bibliothek verfügbar  
The approved original version of this thesis is available in print at TU Wien Bibliothek.



## Chapter 4

# Results and Discussion

The following chapter presents and discusses the results on network length, gas demand and network costs of the developed model. Based on the interpretation of the results recommendation of model improvement are given for further development. A sensitivity analysis of Austrian results shows the influence of a selected set of parameters on the output.

### 4.1 Results for selected Regions in Austria

First, the results of two selected regions in Austria are presented and discussed in detail. One of the regions includes Vienna, the capital of Austria, and the other the city of Graz, which is the second largest city in Austria.

#### 4.1.1 Results of Gas Demand and Network Length Calculation

A significant part of the model's input consists of publicly available open-source data and some of the input parameters are user-defined. The values of the user-defined parameters are based on estimations. In a first attempt, I used so-called standard values with which the first results were calculated. These first results should validate the basic model mechanism. The chosen standard values are listed in Table A.1 in the appendix. Then a sensitivity analysis was performed with the most important input parameters.

The model can estimate the gas demand, the gas network length and the associated costs for gas distribution for each selected NUTS 3 region in EU-27. For model validation, the calculation was carried out in Austrian NUTS 3 region Vienna ("AT130 - Wien") and Graz ("AT221 - Graz"). Figure 4.1 and 4.2 show the trends of the gas demand and the network length from 2020 to 2050 for both scenarios (Gas60, Gas20).

In both Austrian cities and scenarios, the plots show a decrease in gas demand. This is mainly caused by the demand-projection tool and the calculated final energy demand raster. The demand-projection tool assumes renovation of the building stock and implementation of efficiency measures in the heating system until 2050, therefore the total demand for final energy is assumed to decrease over time (Figure 3.17). In the Gas20 scenario, the gas demand decreases even more sharply than in the Gas60 scenario. This results from the lower national share of gas heating in buildings in the Gas20 scenario than in the Gas60 scenario (Figure 3.18).

The trend of the grid length in both figures show a similar picture: In both cities and scenarios, the grid length decreases. Only in the Gas60 scenario, the reduction of the grid length is less pronounced than in the Gas20 scenario. The Gas60 scenario shows a

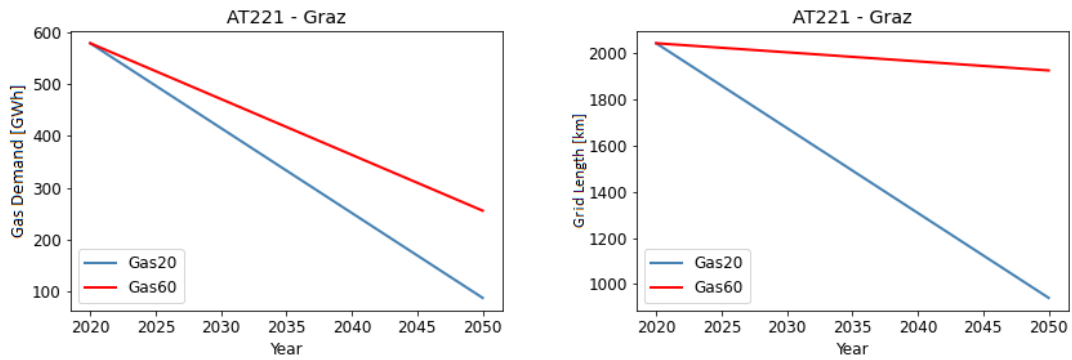


Figure 4.1: Gas demand and grid length of NUTS 3 region Graz

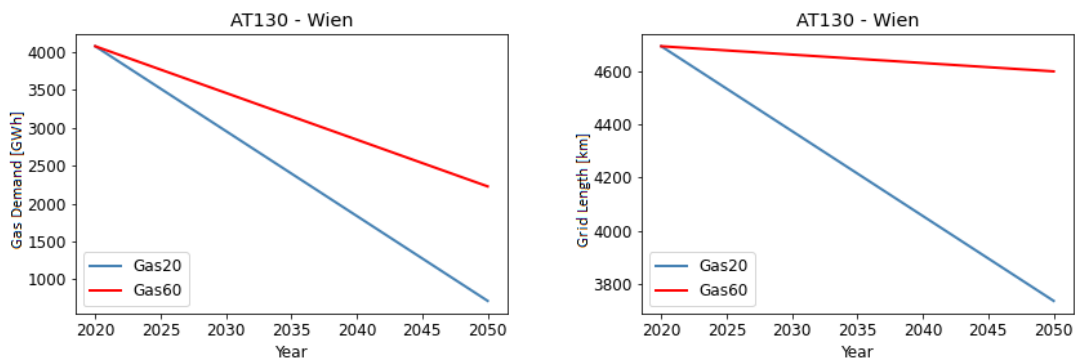


Figure 4.2: Gas demand and grid length of NUTS 3 region Vienna

business-as-usual scenario, where most of the buildings stay connected to the distribution grid. Therefore, the grid length is almost stable. What else happens is, that the reduction of the gas demand in the Gas60 scenario is not caused by consumers disconnecting from the distribution network, but rather by building stock renovations and efficiency measures in the heating systems until 2050.

#### 4.1.2 Results of Network Cost Calculation

The values of the calculated distribution grid length and the gas demand were used for the NPV calculation. Additional parameters for calculating the NPV are listed in Table A.1. The assumed finance strategies of network operators in both scenarios are described in Section 3.7. Figure 4.3 shows the total expenditures per city and scenario.

The gas distribution network in Vienna has expenditures twice as large as in Graz, which is due to the fact, that the calculated network length in Vienna is more than twice as large as the network length in Graz. Comparing the expenses between the individual scenarios, total expenses are slightly lower in the Gas20 scenario than in the Gas60 scenario. This results from the smaller grid length in 2050 in the Gas20 scenario. Expenditures, referring to operational costs and maintenance costs, depend positive on the grid length, therefore these costs are higher in the Gas60 scenarios.

Network revenues are gained from grid charges, which are modelled based on the gas demand, according to Equation 3.27. Comparing the expenditures in Figure 4.3 and the grid charges in Figure 4.4 in each city and scenario, the grid charges do not cover the expenditures. In other words, the assumed grid charges do not cover the assumed costs for

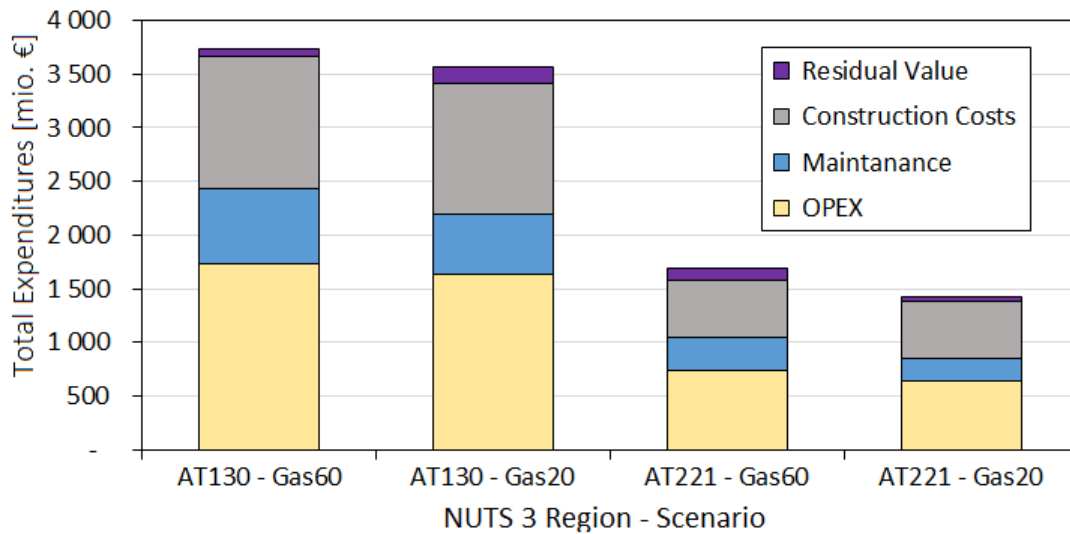


Figure 4.3: Expenditures of the gas distribution networks in Graz and in Vienna

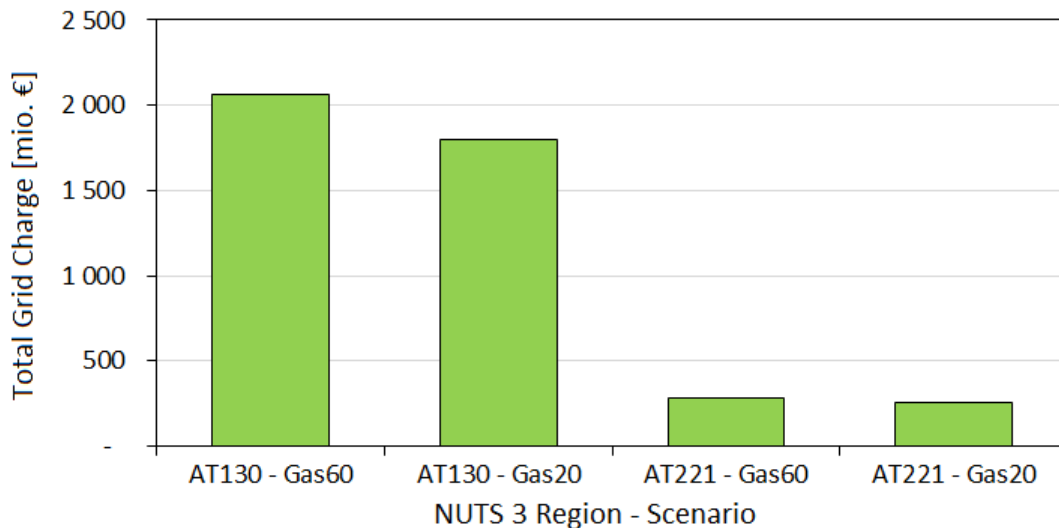


Figure 4.4: Revenues of the gas distribution network in Graz and Vienna

constructing, operating and maintaining the gas distribution networks in both cities until 2050. This is caused by the sharp decline of gas demand in both cities and scenarios due to renovation and efficiency measures in the building stock. If the demand for gas would be kept at a constant level, the grid charges would cover the expenditures in this model. Another way to cover the expenditures would be to raise the grid charges constantly over the years to compensate for the decreasing gas demand.

The NPVs in each city and scenario is calculated by subtracting the expenditures from the revenues. Figure 4.5 shows the resulting NPVs. Under the assumptions of the scenarios, the NPV is negative in all scenarios and cities, concluding that the distribution networks in both cities cannot be operated profitably under the made scenario assumptions. In Vienna, the Gas60 scenario is less unprofitable whereas in Graz the Gas20 scenario is less

unprofitable. This results from the calculated decrease between gas demand and network length. With decreasing network length, expenditures decrease and with decreasing gas demand, revenues decrease until 2050. Concluding, if the network length decreases faster than the gas demand, the network gets more profitable and vice versa.

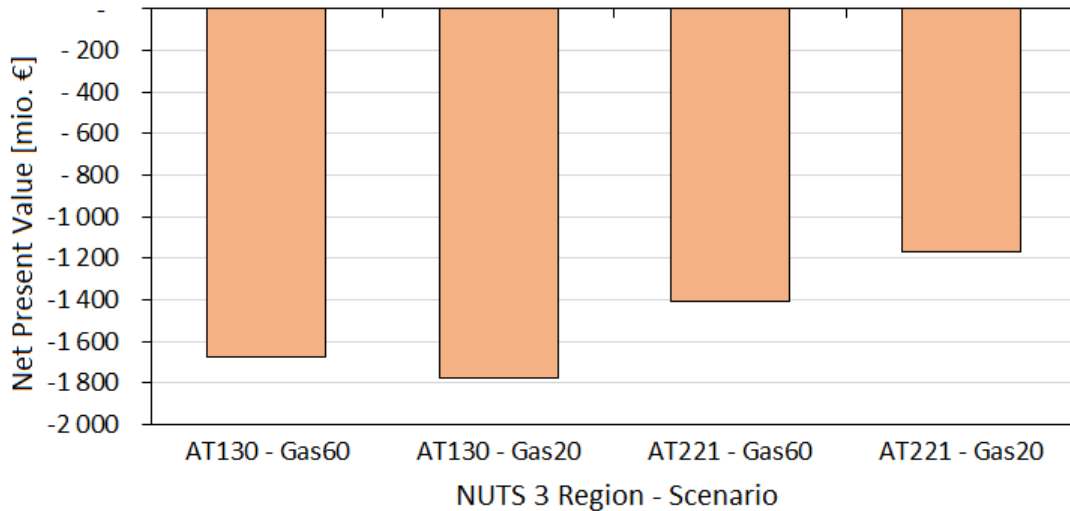


Figure 4.5: Net present value of gas distribution network in Vienna and Graz under assumption of the Gas60 and the Gas20 scenario

## 4.2 Results for EU-27

One of the strengths of the model is its easy computational extensibility over a large number of regions. With some exceptions, the calculation has been performed in all NUTS 3 regions in the EU-27. The standard values in Table A.1 were chosen to serve as input parameters for each country with country-specific values of gas share  $x^{gas}$  and share of district heating  $x^{dh}$  in the supply mix for space heating and hot water preparation. Both values were extracted from the predefined scenarios from the Invert/EE-Lab. Figure 3.18 shows the country-specific share of gas for the years 2020 and 2050 for the scenario Gas60 and Gas20. The share of gas in 2020 is located between 0 % and 83 %. The gas share for the Gas60 scenario is located between 2 % and 32 %, for the Gas20 scenario between 0.7 % and 12.4 %. Both scenarios do not indicate a share of gas in Cyprus in 2020 and 2050. Therefore, Cyprus was excluded from further calculations.

As explained in Chapter 3, the share of gas for each country has been calculated under the assumption that the EU meets the target of a carbon-neutral energy system in 2050 by the Invert/EE-Lab module. More precisely, the module has an overall scenario target of gas heated gross floor area in the EU-27 (60% in Gas60 and 20% in Gas20). Based on the potential of gas heated areas, the gas share has been distributed across all EU countries to meet the scenario target. This results that the gas demand in 2050 increases or decreases related to the gas demand in 2020 based on the chosen scenario and even in countries, where no gas demand exists in 2020 indicating a gas demand in 2050. For example, Malta indicates from 2020 to 2050 an increase of gas share from 0 % to 5 – 7 %, which means the gas distribution network will be extensively expanded until 2050. The same applies to Sweden, Finland and Cyprus. For simplicity, the impact of an extensively growing network on the NPV is not examined in this thesis. Therefore, the mentioned

countries are excluded from further calculations.

Not all buildings in an identified gas distribution network area are connected to the gas network. Therefore the share of connected buildings to gas distribution networks (connection rate,  $x^{gas,n}$ ) in each identified network area is set to the same value in all EU-27 countries. For 2020, the share of connected buildings is set to 60 %, which is the current share. In the Gas60 scenario,  $x^{gas,n}$  is set to 60 % in 2050 whereas in Gas20  $x^{gas,n}$  is set to 20 % in 2050. Thus in the Gas60 scenario, the connection rate is considered to remain the same value from 2020 to 2050. In the Gas20 scenario, the connection rate is considered to decrease by 40 % from 2020 to 2050. Assumptions on gas share changes compared to changes in the connection rate diverge. For example, in some countries, the connection rate remains the same and the gas share to final energy demand increases from 2020 to 2050. Figure 4.6 shows the differences in the assumptions. In 9 out of 23 countries, the share of gas demand decreases less than the connection rate in one or both scenarios. In all other countries, the gas demand is assumed to decrease more than the connection rate.

The figure does not show the full columns for Sweden and Finland. Both countries have an increase of gas share in the final energy demand from 1 % in 2020 to 5 – 12 % in 2050. At the same time, it is assumed, that the connection rate will stay constant in Gas60 and decrease to 33 % in the Gas20 scenario. The relative share of gas demand divided by the relative connection rate gains  $\sim 1000 - 3000$  % in the Gas60 scenario and  $\sim 2000 - 7000$  % for the Gas20 scenario in both countries. That means, the gas demand increases 10 – 70 $\times$  more than the network length, which seems unrealistic. Because of this, the evaluation of Finland and Sweden were excluded too.

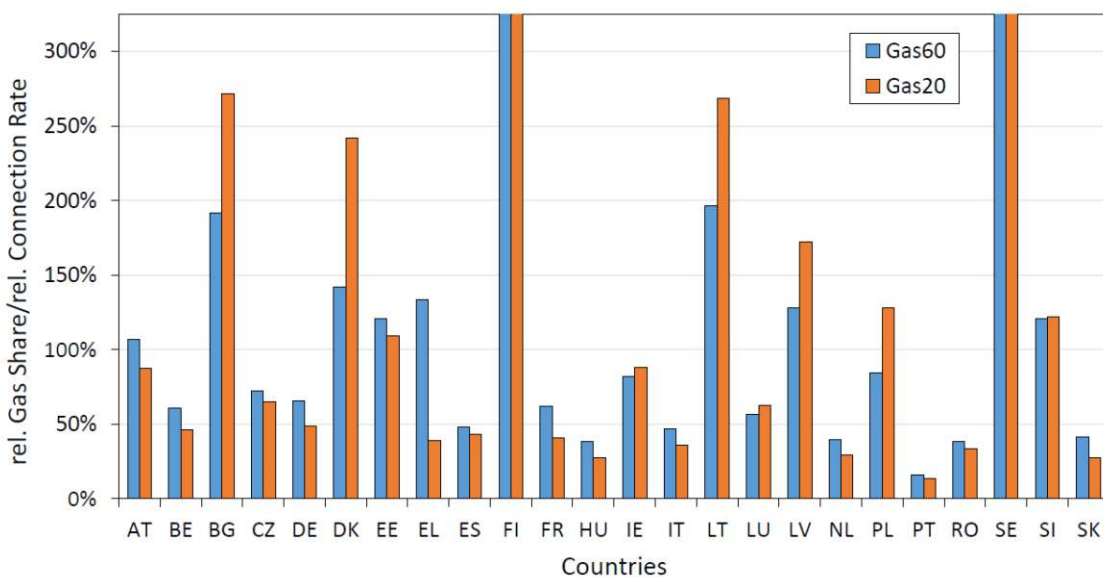


Figure 4.6: Relative share of gas demand related to relative connection rate in each scenario and country

#### 4.2.1 Results of Gas Demand and Network Length Calculation

In the first step, the model evaluated for both scenarios the gas demand in 2020 and 2050. Figure 4.7 shows the distribution of the gas demand in 2050 related to the gas demand in 2020. The figure shows the results for each country and scenario.

In all countries, the gas demand decreases more sharply in the Gas20 scenario than in

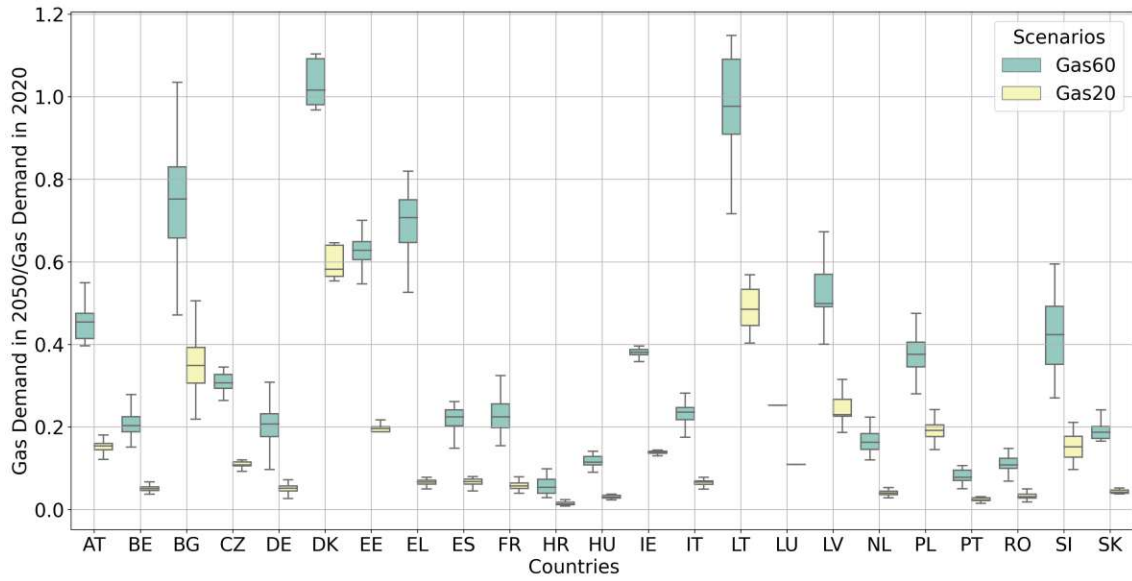


Figure 4.7: Distribution of gas demand in each country in 2050 related to 2020 in both scenarios

Gas60. The median of gas demand related to the year 2020 in Gas60 is distributed around 10 – 100 %, in Gas20 around  $\sim 1 - 60$  %. Some regions in Belgium, Denmark and Latvia expand their gas consumption in buildings for space heating and hot water preparation in Gas60 (Figure 4.7). In all these countries, the share of gas heating and hot water preparation  $x^{gas}$  increases from 2020 to 2050 in Gas60. Luxembourg consists of one NUTS 3 region, therefore, it has no distribution in both figures.

Figure 4.8 shows the distribution of the network length in 2050 related to the network length in 2020 in each country and scenario. The medians of network length in 2050 in Gas60 are around 60 – 90 % related to the network length in 2020. In the Gas20, the medians of the countries are located between 20 – 40 %.

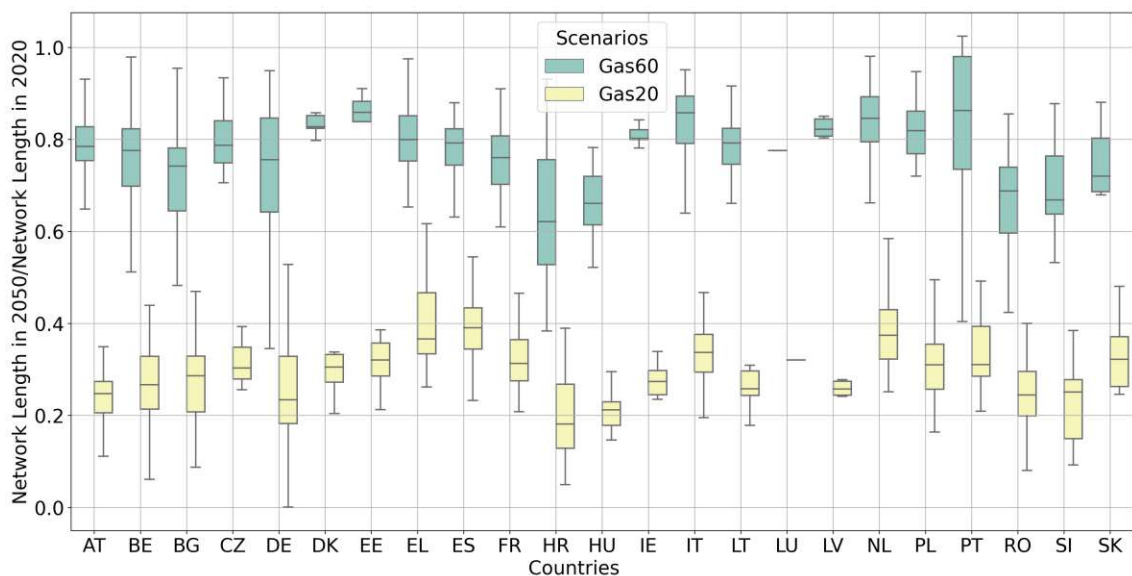


Figure 4.8: Distribution of network length in each country in 2050 related to 2020 in both scenarios

Both last Figures show that parameters gas demand and distribution network length tend to decrease from 2020 to 2050. Depending on the country, gas demand or network length decreases more. Following Figure 4.9 shows the Gas Demand per Network Length (GPN) in 2050 related to GPN in 2020 per country and scenario. The Figure reveals a very different development of the parameter  $GPN$  in 2050/ $GPN$  in 2020 in each country and scenario. In most countries, where the share of gas systems in buildings increases, the gas demand per network length increases too. In all other countries, where the share of gas to the final energy demand slightly increase or decrease, show a decrease in gas demand per network length. Comparing Figure 4.9 and 4.6 shows, that the development of demand per network length strongly correlates with the assumed development of the share of gas systems to connection rate.

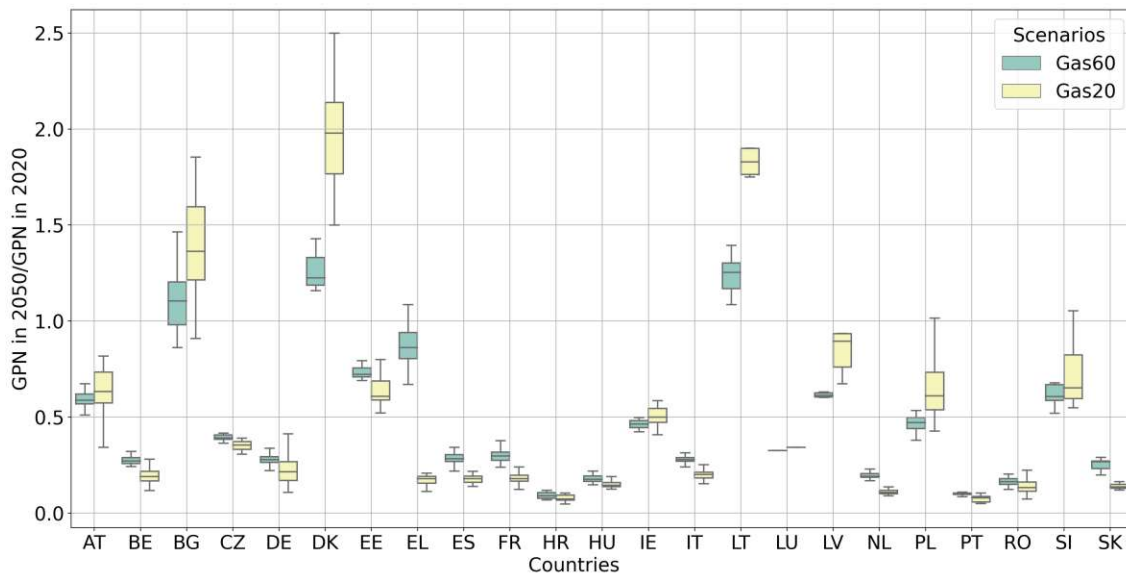


Figure 4.9: Distribution of gas demand per network length in 2050 related to 2020 in both scenarios

The correlation means, that the development of gas demand and network length depends strongly on made assumptions of development of gas share to the final energy demand and development of connection rates. Both parameters are chosen independently. However, an increase of gas demand per network length from 2020 to 2050 with a decrease of network length, would mean, that the gas demand per hectare would increase in the same years. The scenarios generally define a decrease of final energy demand per building due to renovation and efficiency measures in the building stock (Figure 3.17). That means, that buildings would exchange their heating system for gas-based heating systems, especially in Bulgaria, Denmark and Latvia. Figure 4.9 shows, that the gas distribution network will tend to shrink from 2020 to 2050 with more buildings connected making a smaller but denser gas distribution grid. However, connecting more buildings would mean network expansion which is related to investment costs. Currently, costs for expansion are only considered, if the total length of a gas network in a region increases. If the total gas network length of a region decreases but increases in certain hectares, costs for network expansions are not considered but could be implemented in the future.

Furthermore, the development of the connection rate should be correlated to the devel-

opment of the gas share to the final energy demand. As already discussed, Sweden and Finland show a very unrealistic relation of gas share development to connection rate development, which could be avoided by deriving one parameter from the other and creating a relationship between them.

#### 4.2.2 Results of Network Cost Calculation

The calculation of the NPV of assumed gas distribution networks have been performed for 23 EU-countries. As already described, Sweden, Finland, Cyprus and Malta were excluded from the calculation due to the unrealistic assumptions on gas share and connection rate. To compare the NPV of the individual country with each other, the values for the NPV were divided by the number of inhabitants located in gas designated areas. Figure 4.10 shows the NPV until network decommission per capita (2020) in 23 countries and in both scenarios.

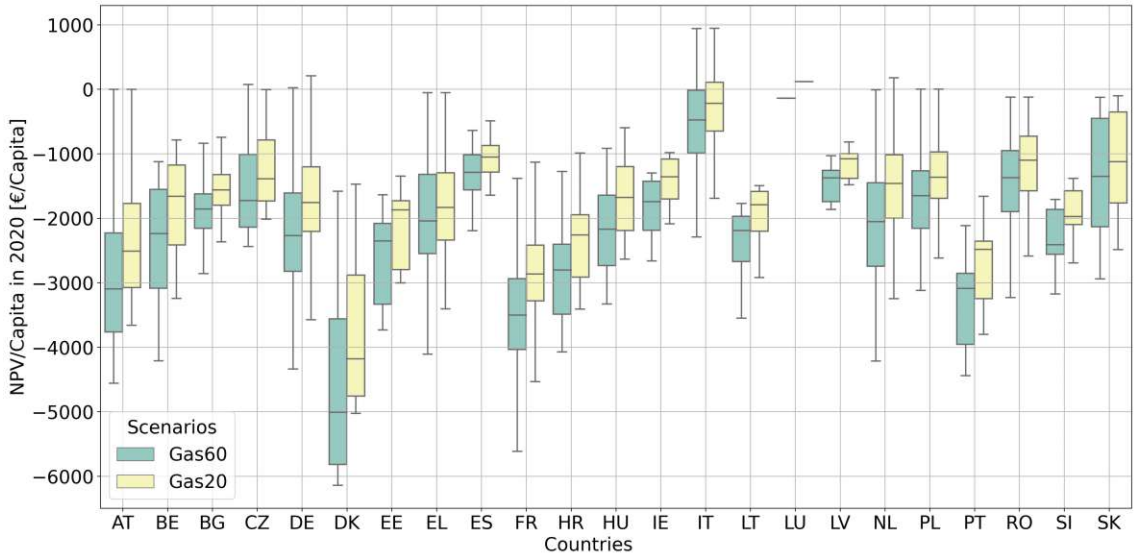


Figure 4.10: Distribution of the NPV, calculated from the construction year until the network decommission, per capita (2020) in both scenarios

With the current choice of input parameters, hardly any network is profitable. Only some regions in the Czech Republic, in Italy and the Netherlands have a NPV above 0 €. Interestingly, as the gas distribution networks have a higher NPV in the Gas20 scenario than in the Gas60 scenario. Considering that the Gas20 scenario is a gas phase-out scenario, it is more economical for a gas network to exit gas shortly after 2050 under the made model assumptions. This fact results from different reasons. The first reason is the differences in the running cost coverage between the assumed scenarios. Running cost coverage is given, when the yearly revenues cover the yearly expenditures, according to

$$\frac{R_t}{C_t} = \frac{E_t \cdot c_{gc}}{c_1 \cdot l_t + c_2 \cdot E_t} = 1 \quad . \quad (4.1)$$

By inserting the parameter values from Table A.1, the equation reduces to

$$\frac{E_t}{l_t} = \frac{c_2}{c_{gc} - c_1} = \sim 0.63 \quad , \quad (4.2)$$



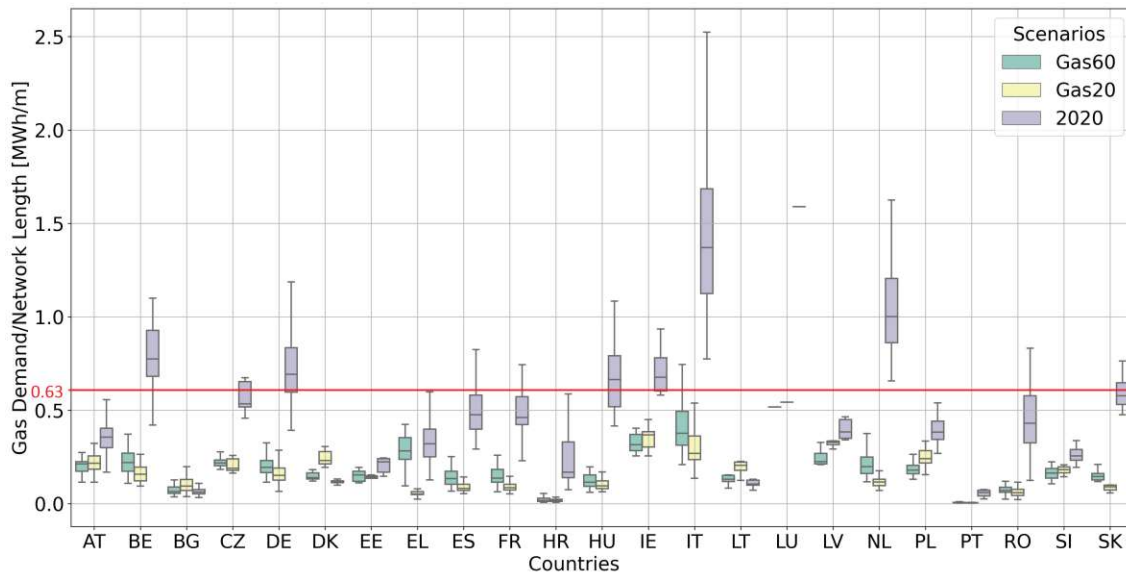


Figure 4.11: Distribution of gas demand per distribution network length in  $MWh/m$  in 2020 and 2050 in both scenarios

which means, a gas distribution network can cover its running costs when the gas demand per network length is above  $0.63 MWh/m$ . Figure 4.11 shows the gas demand per distribution length in  $MWh$  per  $m$  in 2020 and in both scenarios in 2050. The red line at  $0.63 MWh/m$  indicates the minimum gas demand per network length to cover the running costs in the current year.

As clearly visible in the figure, in 7 EU countries running costs are covered by the grid charges in 2020. Since 1990, the gas consumption in households and in the commercial sector has been increasing from  $1100 TWh$  to  $1400 TWh$  in EU-27 [10]. Assuming, that most distribution networks were renovated or built within the last 30 years, they should be profitable at least at the time they were renovated or built. If the gas demand has been increasing since then, model results of lacking network cost coverage seem unrealistic. First of all, the input parameters for the OPEX calculation need to be checked for reasonable values in the literature. If the costs for OPEX are reasonable, the calculation of the network length should be reevaluated. Assuming, that most gas distribution grids were built the last 30 years and grid charges covered running costs at this time, the current model with given input parameters overestimates the gas network length in 2020.

The network length calculation is based on the potential gas share per hectare, which is developed by breaking down the national gas demand to the hectare level. With current standard values (Table A.1), almost every NUTS 3 region in the EU-27 is designated as a gas-consuming region. The model then calculates the length for a supplying gas distribution network. To avoid an overestimation of the gas network length, the value  $h^{\text{cluster}}$  demand for the clustering algorithm could be increased. This value controls, if a cluster has enough potential gas demand to be identified as a cluster with gas consumption, as explained in Section 3.3.4. When increasing this value, fewer regions get designated as gas-consuming ones. The national final energy demand for gas in the building sector is distributed over fewer regions and less gas network length is needed to supply those areas, resulting in regions with a higher gas demand per network length.

Furthermore, the parameter  $d^{eff}$  for calculating the distance probability raster could be

decreased. The parameter determines the maximum distance of a hectare element from the next European transmission line to get designated as a gas-consuming area, as explained in Section 3.3.3. If the parameter  $d^{eff}$  is set to a lower value, fewer clusters are assigned as a gas-consuming cluster. The remaining areas share a higher final energy demand for gas and the gas demand per network length increases.

A further model improvement to tackle the problem of network length over-estimation would be a *costs coverage calculation* of the designated individual clusters. The calculation sorts the clusters by increasing the ratio of gas demand per network length. The clusters that have the lowest ratio of gas demand per network length get unassigned as gas-supplied areas. Afterwards, the gas demand is recalculated over the assigned regions until a fair amount of clusters have a distribution network with a reasonable gas demand per network length in 2020.

When looking at the gas demand per network length in 2050 in Figure 4.11, no country in no scenario can cover the running costs. In some cases, the gas demand per network length in the Gas60 scenario is higher than in the Gas20 scenario. Comparing with Figure 4.6 shows, that this depends strongly on the chosen development of gas share from 2020 to 2050, related to the chosen development of connection rate in the same years. The scenario, which has a higher gas share development per connection rate development, has a higher gas demand per network length in the individual country.

However, the problem of network length overestimation does not fully explain, why the Gas60 scenario has a lower NPV than the Gas20 scenario in all countries (Figure 4.10). Taking a closer look at the running network maintenance costs ( $I_{main,t}$ ) reveals further reasons. These costs depend on the actual network length and user-defined network length specific costs, according to Equation 3.30. From 2020 until 2034, these costs are fully spent ( $irf_t=1$ ) in each scenario to keep the average asset age at a constant level. From 2035, the model changes the investment strategy of the network operators. As explained in Section 3.6, from 2035 the expenditures for network asset maintenance decrease by factor  $irf_t < 1$ . This continuously decreases the average asset age of the network over the years to reach a user-defined average asset age in 2060. In the Gas20 scenario, the parameter  $irf_t$  is chosen, so that the network reaches a  $MRBVF_t$  below 0.25 and in the Gas60 scenario a  $MRBVF_t$  below 0.5 in 2060. To reach a lower  $MRBVF_t$  in 2060,  $irf_t$  is lower in the Gas20 scenario than in the Gas60 scenario, leading to fewer maintenance costs per year in the Gas20 scenario. The total costs for maintenance per scenario are shown in Figure 4.12.

In the Gas20 scenario, the regions have an average investment reduction factor  $irf_t$  of  $\sim 0.5$ , in the Gas60 scenario an  $irf_t$  of  $\sim 0.8$ . The Figure clearly shows the higher maintenance costs in Gas60 scenario, which results in a lower NPV per capita (Figure 4.10). Model improvements regarding the maintenance cost can be made by correlating the investment reduction factor  $irf_t$  with network revenues and expenditures according to

$$\frac{R_t}{OPEX_t + I_{main,t} \cdot irf_t} \geq 1 \quad (4.3)$$

with  $max(irf_t)$  of 1. Thus, the model spends on maintenance what is covered by the annual income.

The calculation of the residual value  $RV$  depends on the yearly revenues and operational costs after 2050 and thus on the gas demand per network length in 2050. If gas demand per network length is below  $0.63 \text{ MWh}/m$  in 2050, the residual value is negative in each year after 2050 until network decommission. In the Gas20 scenario, the model decommissions

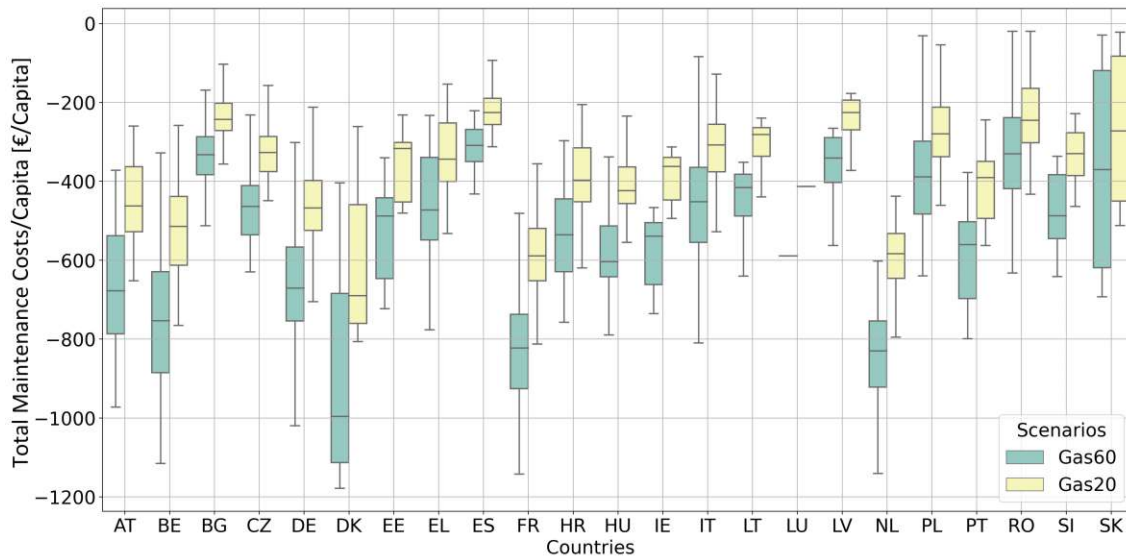


Figure 4.12: Distribution of maintenance costs per capita in €/capita from 2020 to 2050 in both scenarios

most networks in 2061, in the Gas60 in 2065. The current model calculates a gas demand per network length in 2050 in both scenarios below 0.63, thus both scenarios have a negative residual value. In the Gas60 scenario, these negative costs are spent mostly 15 years, from 2050 until 2065. In the Gas20 scenario mostly 11 years, from 2050 until 2061. This leads to higher negative residual values in the Gas60 scenario than in the Gas20 scenario (Figure 4.13).

The residual value in the network cost calculation should reflect the remaining economic value of the distribution network in 2050, based on grid charges and OPEX. If the grid charges can not cover the operational costs in 2050, each year after 2050 would be an economic loss. Therefore, model improvements regarding the residual value calculation can be made by only considering the residual value if the grid charges cover the OPEX in 2050. Else the network is given a defined time after 2050 until decommission, which should simulate the time where gas consumers can switch to alternative applications and gas lines can be closed step by step.

### 4.2.3 Allocation of potential Gas Distribution Networks

Based on the input parameters, the model calculates the potential gas network length and gas demand in a selected region. The results vary with respect to the scenario and year. Figure 4.14 shows in a map of EU-27 the calculated model results of each region, visualised in a certain colour. The colour indicates whether or not a gas distribution network potentially exists in a specific year and scenario. Regions that are marked dark blue potentially utilise gas distribution networks in 2020 and 2050 in both scenarios. The regions in red contain potential networks in 2020 but 2050 only in the Gas60 scenario. Regions that utilise potential gas distribution networks in the Gas20 scenario but not in the Gas60 scenario do not exist. Some regions exist that contains potential gas distribution networks in 2020, but none in 2050 in both scenarios. These are marked pink in Figure 4.14. The networks in these regions are modelled with a linear decrease of gas demand and network length until both values are 0 in 2050, assuming a decommissioned network in 2050. However, the network may have been closed at some point long before 2050 - and not in 2050. The model could be improved by calculating the network cost calculation

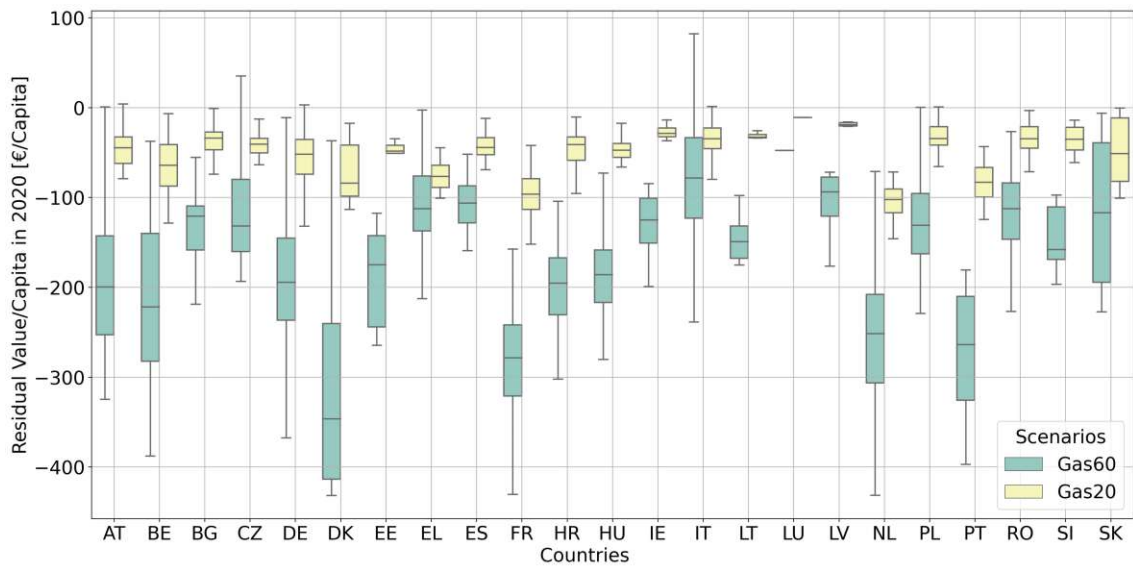


Figure 4.13: Distribution of residual value per capita in €/capita from 2050 to year of decommission in both scenarios

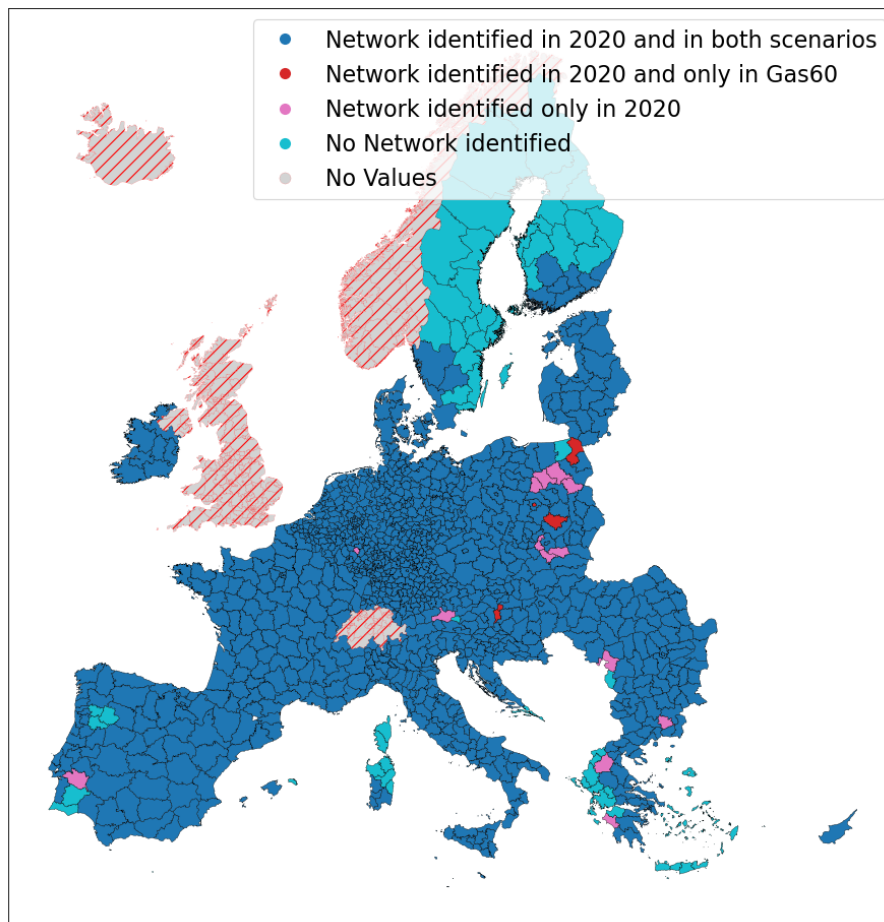


Figure 4.14: Identified gas distribution networks in each region, year and scenario

until the year when grid charges do not cover operational costs anymore. This year could be assigned as the year of decommissioning.

Cyan regions indicate areas, where the model calculates no potential gas supply in 2020 and 2050. Especially Finland and Sweden contain such regions. The reason for that lies in the distance to the next European transmission line. All these regions, most of them in the north and some in the south are further away than 50 km from the nearest transmission line, therefore no gas distribution network is indicated. If the parameter  $d^{eff}$  is set to a lower value than 50 km, the number of regions with no distribution network increases. Grey and red crossed countries are not included in the model calculation (UK, Iceland, Norway, Switzerland).

### 4.3 Sensitivity Analysis

A sensitivity analysis was performed to measure the sensitivity of the model's output variable. The analysis examines the uncertainty of the results due to the uncertainty of the input parameters. To perform the analysis, chosen input parameters were changed by +10 %, +20 %, -10 % and -20 %. Further, the results for each input parameter variation were calculated. The mean value of the results across all regions in a country was calculated and plotted per chosen parameter.

A set of parameters was used to calculate the sensitivity of gas demand and the network length for all NUTS 3 regions in Austria. The same was performed for the NPV calculation sensitivity.

#### 4.3.1 Sensitivity Analysis of Network and Demand Estimation

Figure 4.15 and 4.16 show the results of the sensitivity analysis of the network length and gas demand calculation. A set of eleven input parameters was chosen to examine the variation of results.

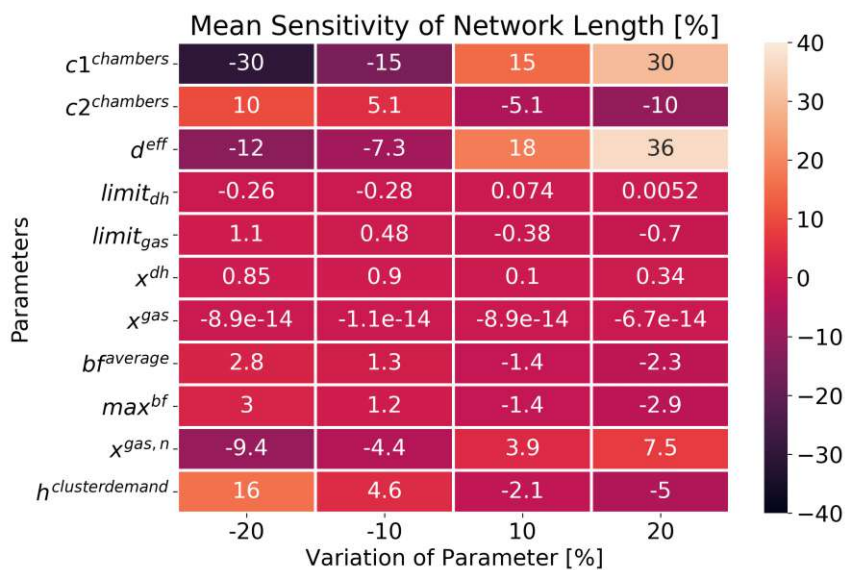


Figure 4.15: Mean sensitivity of the network length calculation in percent per parameter

Each chosen input parameter has an influence on the resulting network length to a smaller

or wider extent. The parameters in Equation 3.17 correlate positive ( $c1^{chambers}$ ) and negative ( $c2^{chambers}$ ). However, these input parameters are fixed by findings of [27]. The effective distance  $d^{eff}$  correlates positively with the resulting mean network length and mean gas demand. Looking at the mean sensitivity for both results, the mean network length changes by +18 %, the mean gas demand by +130 % when changing the effective distance by +10 %. Any hectare element, that is more than  $d^{eff} * 100$  Meters away from the transmission network, gets excluded. Extending or reducing this limit can lead to opening up or closing parts of heat demand and building clusters for network length and gas demand calculation. An improvement that can be made here is for example adapting the calculation of the related connection potential  $w_{i,j}^{con}$ , which depends on  $d^{eff}$ . Currently, each hectare element within an identified cluster has a different connection potential, depending on their respective distance to the transmission line. A part of a cluster could be disconnected from the distribution grid if the distance from the transmission network for respective hectares is greater than the chosen effective distance. In general, it makes more sense if the connection potential of the entire cluster has the maximum or means value of the connection potential  $w_{i,j}^{con}$  within the cluster to avoid parts of the cluster being disconnected.

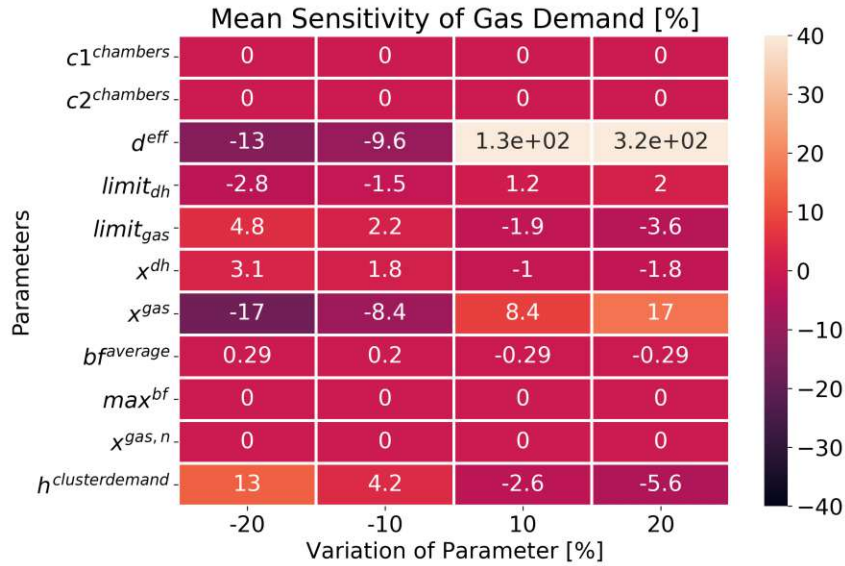


Figure 4.16: Mean sensitivity of the gas demand calculation in percent per parameter

Variation of parameters  $limit_{dh}$ ,  $limit_{gas}$ ,  $x^{dh}$  and  $x^{gas}$  have little impact on the resulting mean network length but a greater impact on the resulting mean gas demand. Especially variation of  $x^{gas}$  has hardly any impact on the resulting mean network length. The sensitivity of the network length correlates with parameter  $x^{gas,n}$ . Both parameters ( $x^{gas}$  and  $x^{gas,n}$ ) are predefined from the scenario from Invert/EE-Lab [31].

The parameter  $h^{clusterdemand}$  has approximately the same impact on the mean gas demand and mean network length and correlates positively to each of them.  $c1^{chambers}$ ,  $c2^{chambers}$ ,  $max^{bf}$  and  $x^{gas,n}$  have no impact on the mean gas demand. These parameters only influence the estimation of the network length.

### 4.3.2 Sensitivity Analysis of NPV Calculation

Figure 4.17 shows the mean sensitivity of the NPV calculation. Parameter  $c_1$  and  $c_2$  are used for calculating the OPEX (Equation 3.29). The mean sensitivity of the NPV by variations of parameter  $c_1$ , which scales with costs per network length, is much larger than by variation of parameter  $c_2$ , which scales with costs per amount of gas flowing through the network. The NPV's sensitivity correlates positively with network length variation  $l^{building,gas}$  and negatively with gas demand variation  $E^{building,gas}$ , whereas the negative correlation with the network length variation is higher than the positive correlation with the gas demand variation.

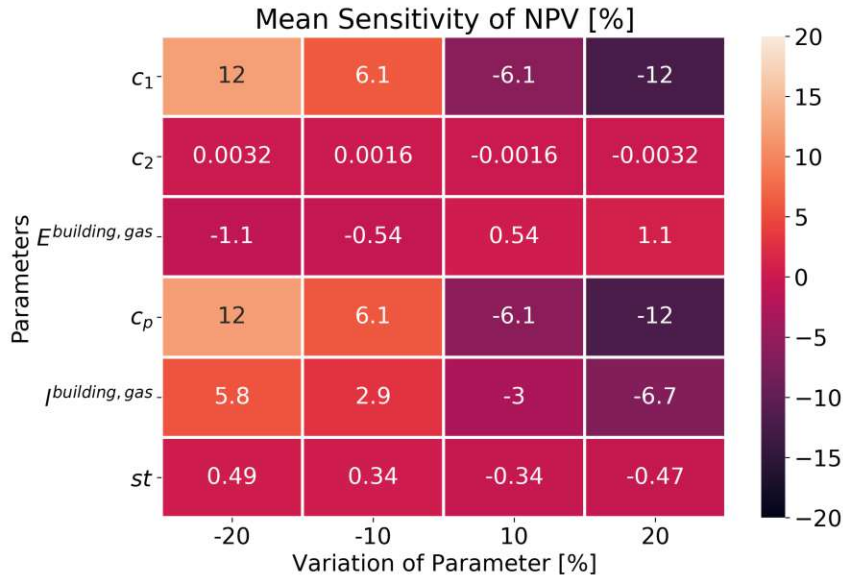


Figure 4.17: Mean sensitivity of the NPV calculation in percent per parameter

The investment costs per network length  $c_p$  correlate negatively with the mean sensitivity of NPV. If the length specific costs for the network increase, the NPV decreases, resulting from increasing construction and maintenance costs. Each distribution network in Austria experiences a reduction in network length in each scenario. The investment costs of decommissioned lines before their end of service time are considered sunken costs. If decommissioned lines can be used for another purpose in a profitable manner, it would bring an added value to the NPV.

The impact of service time variation  $st$  on the mean sensitivity of NPV calculation is very low. This means, expanding the lifetime of network assets would not significantly affect the profitability of the network.

## 4.4 Validation of Results - Comparison with real Data

To validate the model, the calculated results of selected regions were compared to real network data provided by the respective district network operator: Vienna with a total distribution grid length of approximately 4700 km [45] and a total gas demand for households around 5200 GWh [46] and Graz with a total network length of approximately 600 km [47] and a total gas demand around 1000 GWh [47]. Data is provided without any further specifications. Therefore it is not known, whether the total length specifications consist of the length of a high-pressure network (e.g. for industries), or if the gas demand

specifications include gas demand for industries. Currently, the model takes into account the building sector but not the industrial sector. Thus, these provided values can be considered as upper limits. Both results match in the order of magnitude, whereas the data for Vienna are more in-line with model results. For Graz, the model seems to overestimate the gas demand and the network length (Table 4.1). In both cases, the input parameters still need to be adapted. However, this is outside the scope of this work.

Table 4.1: Comparison of model results with real network data

	Region	Vienna	Graz
real Values	Gas Demand [GWh]	5200	1000
	Network Length [km]	4700	600
calculated Values	Gas Demand [GWh]	4070	580
	Network Length [km]	4350	1400

## 4.5 Model Perspective

Currently, the gas network model is in a very basic state. It can calculate the potential gas demand and network length to supply a set of buildings in the building sector in each NUTS 3 region. The calculation is based on geographically localised building data, network data, data on final energy demand and assumptions about various sets of parameters. Based on the gas demand and the network length, the model calculates the associated NPV of networks in a NUTS 3 region. The model has implemented a gas demand and supplying network length calculation module of European gas power plants based on the localisation and capacity of each gas power plant. However, the module has not yet been used. In that state, the model can answer questions about the distribution of potential gas networks, gas demand and associated costs for supplying buildings with gas over Europe. Furthermore, it can assess the impact of renovation and efficiency measures in the building stock on the local gas distribution structure and its related costs.

Recommendations for model improvement, such as adaption of input parameters, modification of methodology, etc. are given based on the results. These recommendations do not include any improvements regarding the scope of the model. Therefore, the following paragraphs are intended to discuss possible features that extend the model's functionality. However, the paragraphs will not be detailed step-by-step instructions on how to implement these features, but rather explain and discuss the implementations abstractly. Both the details of such features and their implementation have been already discussed and described in various sources and will therefore not be analysed.

Figure 4.18 gives a comprehensive overview of a possible future model and its implemented features to expand the model's scope. The light blue coloured shapes are exemplary NUTS 3 regions. The values for each region are currently calculated independently from each other. Implementing the current model in a **node-edge model** would establish functional relations between the regions. Such an exemplary node-edge model is shown in Figure 4.18. The purple nodes are the centre of each region and contain information like the regional gas demand as well as the gas network length. Each node is then connected via a brown edge with other nodes. The edges illustrate the functions and the dependencies the nodes have to each other. Generally, these dependencies simulate the **transport capacities** of gas in a supra-regional gas network to transmit the gas from the European transmission network to the regional distribution networks. Furthermore, a supra-regional gas network enables transport between these regions. As a result, these dependencies are



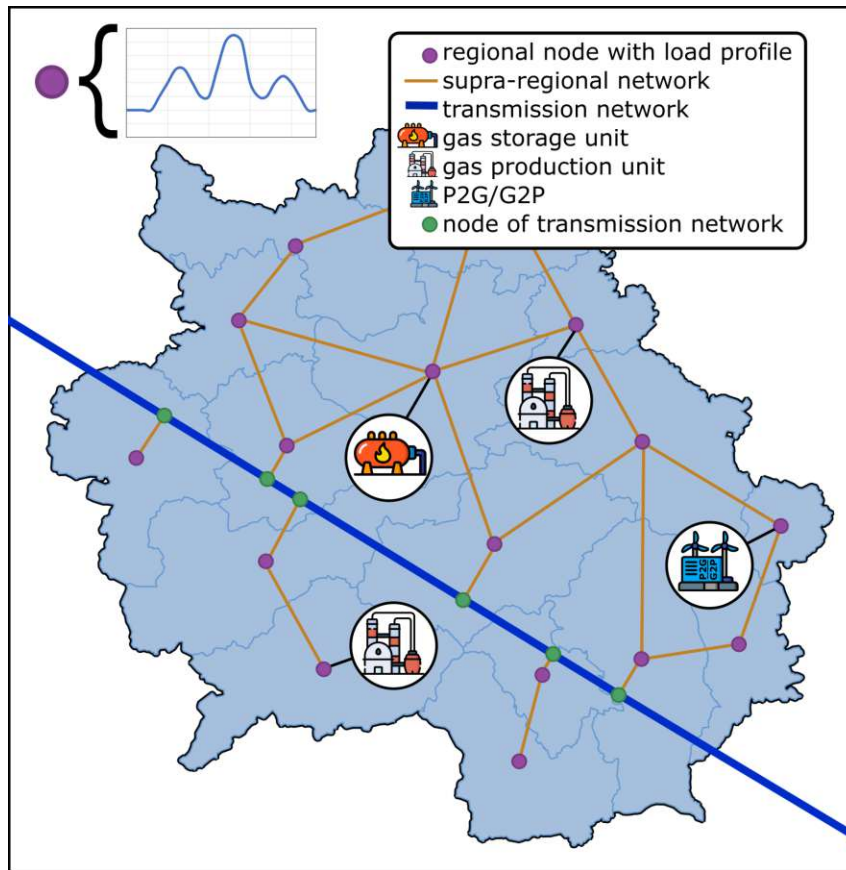


Figure 4.18: Future perspective of the open-source gas model<sup>1</sup>

mostly based on pipe, gas or other transport equations. The European transmission network is displayed as the dark blue line crossing through region (Figure 4.18).

This implementation would shift the model from a **regional-centred cash-flow model** to an **infrastructure model**. On the one hand, such an infrastructure model can answer questions regarding the transport capacity of the supra-regional network. For example, each node's gas demand is combined with a **time-specific load profile** to distribute the gas demand throughout a defined period. Thus, the model can identify capacity limitations in the gas supplying infrastructure at a defined time. An exemplary node's load profile is shown in the line plot in the upper left corner of the Figure 4.18. On the other hand, such an implementation would open up many new questions that need to be addressed before the feature implementation. Since there is no publicly available information about supra-regional gas network location and capacity, the connection of the nodes is based on estimations. Figure 4.18 shows such an estimation, where the nodes that are directly adjacent to the European transmission network are connected to it. All other nodes are connected to those nodes closest to them. This task might be part of the already mentioned minimum-tree-spanning problem and can be solved by the Kruskal algorithm [40], which finds the shortest connection between a set of nodes. The location of possible supply bottlenecks mostly depends on the location of the generated edges, which connect the nodes.

Another question that needs to be answered before implementing a node-edge model is the role of the European transmission network. The European transmission network expands

<sup>1</sup>This Figure has been designed using resources from Flaticon.com

over whole Europe and is supplied by gas from EU- or foreign countries. Natural gas is delivered gaseous via pipeline. The gas flow through the European network is driven by various parameters and is difficult to estimate. Macroeconomic drivers like the price- and demand trends or secret long-term contracts between players in the gas market make it difficult to model this system. Plenty of models already exists that deal intensively with this problem. Therefore, the perspective of this work focus less on the European-wide aspects of gas network modelling but more on a regional or country level.

With that focus, the role of the European transmission network is seen as an **infinite source of gas supply with a predefined price profile and supply capacity per connection node** to the European transmission network. In the next step, further utilities could be implemented in the regional nodes. For example, **gas storage facilities** are a crucial part of the current gas network. Generally, they serve to balance the time-dependent differences between the demand and supply of gas. In the future, their importance could even increase when the share of other facilities, like power-to-gas facilities or other production units, produce gas directly in the country.

Finally, the node-edge model could be implemented in a **cost- and/or flow-optimisation algorithm**. The gas flow between the regions could be simulated at any given point in time, based on assumptions of load profiles, price and demand trends, etc. By coupling the gas model with other existing open-source energy models, the model can be converted into a **complete energy model** where questions about cross-sector coupling effects can be answered.

## Chapter 5

# Conclusion and Outlook

Within the developed gas grid model the gas demand, network length and associated costs for distribution grids in selected regions were calculated. The calculation is based on open-source data and estimations of input parameters. A sensitivity analysis helped to conduct net present value calculations. Further, the mean sensitivity of calculated values from Austrian NUTS 3 regions was plotted. Finally, the resulting network length and gas demand of selected regions were compared to real data provided on the website of district network operators. Partially the results and the available data show good consistency in the order of magnitude, partially the model overestimates demand and network length. Furthermore, the model calculates a decrease in network length and gas demand by the end of 2050 which is in line with scenario assumptions.

### 5.1 Modelling

One of the key findings of this thesis is the difficulty of gas grid modelling. District network operators are not obligated to publish network data like existing network length or the amount of gas flowing through the network. Thus, technical data about the gas network is hardly available. For this reason, the results of gas network models depend remarkably on the assumptions related to the stated parameters. The model becomes as good as the quality of the initial assumptions and input data. To improve the validity of gas demand, network length and network cost estimation, the presented thesis contains several recommendations on model adaptations in Chapter 4. Furthermore, it was discussed how the model and its objective could be expanded. Increasing the model's scope (from regional to country level) would further make the modelling approach a complicated task, but could enable a deeper insight into the gas market.

### 5.2 Results and future Profitability

Another key finding is the effect of decreasing gas demand on the profitability of distribution grids. Even under the continuation of gas heating in buildings under the Gas60 assumptions, distribution grids will experience sharp declines in gas demand, due to renovation and efficient measures in the building stock. Strategies of network operators, which counteract this trend, need to be analysed. One possibility is to increase grid charges and therefore revenues of a network to cover costs. On the one hand, this measure increases the revenues of network operators. On the other hand, this measure can lead to an increasing number of customers leaving the network and changing to a cheaper available heating system, speeding up the decrease of gas demand.

In some cases, decommissioning of network lines could bring added value to the prof-

itability of the distribution network. Reduction in network length will result in reduced operational costs. At the same time, gas consumers will be disconnected and gas demand will decrease. Decreasing gas demand will have the effect of decreasing revenues, due to fewer consumers paying grid charges. The key is only to close network lines, where the sum of grid charges has no significant share to network revenues. Therefore, decommissioning network lines can be an option to counteract the trend of decreasing profitability of gas distribution networks. This can go as far as shutting down the whole grid and managing a controlled face out of gas after 2050 to minimise the economic stranded costs.

Under scenario assumptions of building stock renovation and system-wide exchange of heating systems, the business model for district network operators is tackled. Even when grid charges are increased or network length is reduced to counteract this trend, effects can lead to further consumers leaving the network, resulting in network assets that are stranded or devalued in the medium or long term. Network operators need adequate strategies to either create a gas phase-out that results in the least amount of loss for stakeholders involved or to stabilise the profitability of the district gas network in the long term.

The currently developed model has demonstrated first results, which identifies obstacles gas distribution network operators could experience with used scenario assumptions. However additional studies are needed to evaluate the strategies that DNOs can set to avoid assets being stranded. A further improvement of the current model could help to answer these questions.

# Appendices



Die approbierte gedruckte Originalversion dieser Diplomarbeit ist an der TU Wien Bibliothek verfügbar  
The approved original version of this thesis is available in print at TU Wien Bibliothek.

# Appendix A

## Standard Values

Table A.1: Standard Values for standard Results

Parameter	Description	Unit	Value
<b>Network Costs Estimation</b>			
$i$	calculatory interest rate	%	2
$c_{gc}$	grid charges in base year [48]	€/MWh	17
$r_{gc}$	rate of price increase for grid charges	€/MWh	0
$c_1$	cost parameter for OPEX [1]	€/m	10.71
$c_2$	cost parameter for OPEX [1]	€/MWh	0.012
$r_c$	rate of price increase for OPEX	%	0
$c_p$	cost per length distribution network [1]	€/m	214
$st$	service time of network	years	30
network age	average age of network in base year	years	10
<b>Length and Demand Estimation of Gas Networks</b>			
$abf$	maximum building footprint per building	m <sup>2</sup>	2000
$bf^{average}$	average building footprint per building	m <sup>2</sup>	200
$n^{building,min}$	minimum building per hectare	1/ha	1
$x^{gas,n}$	national share buildings connected to gas distribution network	%	defined by scenario
$x^{dh}$	national share of district heating	%	defined by scenario
$x^{gas}$	national share of gas heating	%	defined by scenario
$limit_{dh}$	limit for full supply of district heating	MWh/ha	500
$limit_{gas}$	limit for full supply of heating by gas	MWh/ha	300
$h^{full\ load}$	fullload hours for gas power plants	h	1000
$\eta^{full\ load}$	efficiency of gas power plant	%	30
<b>Clustering</b>			
EPS	parameter for function DBSCAN	1	1
minPts	parameter for function DBSCAN	1	5
$h^{cluster\ demand}$	demand minimum for identification as a cluster	GWh	12
<b>Calculation of Connection Probability</b>			
$d^{eff}$	distance, where probability is equal 0	100 meter	500

Table A.2: Values of respective scenarios for Austria

Parameter	Description	Unit	Value
<b>Scenario Parameters</b>			
$x^{gas,n}$ (base year)	national share buildings with gas in base year	%	60
$x^{gas,n}$ (Gas60)	national share buildings with gas in scenario Gas60	%	60
$x^{gas,n}$ (Gas20)	national share buildings with gas in scenario Gas20	%	20
$x^{dh}$ (base year)	national share of district heating in base year	%	21.4
$x^{dh}$ (Gas60)	national share of district heating for Gas60	%	14.3
$x^{dh}$ (Gas20)	national share of district heating for Gas20	%	12
$x^{gas}$ (base year)	national share of gas heating in base year	%	23.6
$x^{gas}$ (Gas60)	national share of gas heating for Gas60	%	25.14
$x^{gas}$ (Gas20)	national share of gas heating for Gas20	%	6.9



# List of Tables

4.1	Comparison of model results with real network data . . . . .	50
A.1	Standard Values for standard Results . . . . .	57
A.2	Values of respective scenarios for Austria . . . . .	58



Die approbierte gedruckte Originalversion dieser Diplomarbeit ist an der TU Wien Bibliothek verfügbar  
The approved original version of this thesis is available in print at TU Wien Bibliothek.

# List of Figures

1.1	Correlation between GHG emission reduction and type of gas until 2050 [11]	2
2.1	Economic factors of operating a gas infrastructure . . . . .	7
3.1	General description of the developed OGIS model . . . . .	12
3.2	Final energy demand of Austrian city of Vienna for 2015 (left) and projected for year 2050 (right) . . . . .	14
3.3	Total final energy demand of Austrian city of Vienna $h^{fed}$ (left) and derived final energy demand covered by district heating $h^{fed,dh}$ (right) . . . . .	15
3.4	Illustration of parameters EPS and minPts in python module DBSCAN [33]	16
3.5	Illustration of clustering of hectare elements with dummy values for final energy demand in a $100 \times 100 \text{ m}$ raster . . . . .	17
3.6	Unclustered final energy demand of Austrian city of Vienna $h^{fed,rest}$ (left) and clustered final energy demand of same city $h^{fed,clustered}$ (right) . . . . .	17
3.7	A section of the ENTSOG Transmission Capacity Map 2019 [34]	19
3.8	Workflow from the SciGrid_gas map into a connection probability raster . . . . .	20
3.9	Clustered final energy demand $h^{fed,clustered}$ of Vienna (left) and final energy demand of same city covered by gas $h_{i,j}^{fed,gas}$ (right) . . . . .	20
3.10	Yellow lines indicate the summation border of the NUTS3 region . . . . .	21
3.11	Workflow of generating the <i>number-of-buildings-per-hectare</i> raster . . . . .	22
3.12	OSM section of Vienna, overlaid with <i>number-of-buildings-per-hectare</i> raster (grey-scaled raster) . . . . .	23
3.13	Exponential model fit based on the minimum pipe length as a function of numbers of buildings per hectare [27] . . . . .	25
3.14	Total length calculation of the transmission network . . . . .	26
3.15	Assumed development of gas demand and distribution network length over the service life of a network . . . . .	27
3.16	Share of unrenovated, renovated and demolished gross floor area from 2020 to 2050 per scenario and construction period . . . . .	31
3.17	Final energy demand for space heating in year, scenario and construction period. . . . .	32
3.18	National share of gas in the supply mix for space heating and hot water preparation for each country in EU-27 . . . . .	32
4.1	Gas demand and grid length of NUTS 3 region Graz . . . . .	36
4.2	Gas demand and grid length of NUTS 3 region Vienna . . . . .	36
4.3	Expenditures of the gas distribution networks in Graz and in Vienna . . . . .	37
4.4	Revenues of the gas distribution network in Graz and Vienna . . . . .	37
4.5	Net present value of gas distribution network in Vienna and Graz under assumption of the Gas60 and the Gas20 scenario . . . . .	38
4.6	Relative share of gas demand related to relative connection rate in each scenario and country . . . . .	39

4.7	Distribution of gas demand in each country in 2050 related to 2020 in both scenarios . . . . .	40
4.8	Distribution of network length in each country in 2050 related to 2020 in both scenarios . . . . .	40
4.9	Distribution of gas demand per network length in 2050 related to 2020 in both scenarios . . . . .	41
4.10	Distribution of the NPV, calculated from the construction year until the network decommission, per capita (2020) in both scenarios . . . . .	42
4.11	Distribution of gas demand per distribution network length in <i>MWh/m</i> in 2020 and 2050 in both scenarios . . . . .	43
4.12	Distribution of maintenance costs per capita in €/capita from 2020 to 2050 in both scenarios . . . . .	45
4.13	Distribution of residual value per capita in €/capita from 2050 to year of decommission in both scenarios . . . . .	46
4.14	Identified gas distribution networks in each region, year and scenario . . . .	46
4.15	Mean sensitivity of the network length calculation in percent per parameter	47
4.16	Mean sensitivity of the gas demand calculation in percent per parameter . .	48
4.17	Mean sensitivity of the NPV calculation in percent per parameter . . . . .	49
4.18	Future perspective of the open-source gas model <sup>1</sup> . . . . .	51

# References

- [1] Daniel Then et al. “Impact of Natural Gas Distribution Network Structure and Operator Strategies on Grid Economy in Face of Decreasing Demand”. In: *Energies* 13.3 (Feb. 4, 2020). Number: 3, p. 664. ISSN: 1996-1073. DOI: 10.3390/en13030664. URL: <https://www.mdpi.com/1996-1073/13/3/664> (visited on 07/21/2021).
- [2] Tersteegen et al. *Potentials and levels for the electrification of space heating in buildings - 2nd interim report*. 2022.
- [3] IPCC - *Climate Change 2021 - The Physical Science Basis*. Full Report 6. Issue: 6. IPCC, Aug. 7, 2021. URL: [https://www.ipcc.ch/report/ar6/wg1/downloads/report/IPCC\\_AR6\\_WGI\\_Full\\_Report\\_smaller.pdf](https://www.ipcc.ch/report/ar6/wg1/downloads/report/IPCC_AR6_WGI_Full_Report_smaller.pdf) (visited on 10/08/2021).
- [4] European Commission. *A Clean Planet for all - A European strategic long-term vision for a prosperous, modern, competitive and climate neutral economy*. Brussels: European Commission, Nov. 28, 2018, p. 25. URL: <https://eur-lex.europa.eu/legal-content/EN/TXT/PDF/?uri=CELEX:52018DC0773&from=EN> (visited on 10/11/2021).
- [5] European Commission. *In Depth Analysis - A Clean Planet for all*. Brussels: European Commission, Nov. 28, 2018, p. 393. URL: [https://ec.europa.eu/clima/system/files/2018-11/com\\_2018\\_733\\_analysis\\_in\\_support\\_en\\_0.pdf](https://ec.europa.eu/clima/system/files/2018-11/com_2018_733_analysis_in_support_en_0.pdf) (visited on 10/11/2021).
- [6] Equinor. *Energy Perspectives - Long-term macro and market outlook*. 2021. URL: <https://www.equinor.com/en/sustainability/energy-perspectives.html#> (visited on 10/12/2021).
- [7] Shell. *Sky scenario - Meeting the goals of the Paris Agreement - an overview*. 2018. URL: <https://tinyurl.com/4dbvy5eb> (visited on 10/12/2021).
- [8] “Energy Technology Perspectives 2020”. In: *Energy Technology Perspectives (2020)*, p. 400.
- [9] Felix Chr. Matthes et al. *The Vision Scenario for the European Union - 2017 Update for the EU-28*. Berlin: Öko-Institut e.V, Feb. 2018. URL: [https://www.oeko.de/fileadmin/oekodoc/Vision\\_Scenario\\_EU-28-Report\\_2017.pdf](https://www.oeko.de/fileadmin/oekodoc/Vision_Scenario_EU-28-Report_2017.pdf) (visited on 10/12/2021).
- [10] European Union. *Eurostat - Data Explorer*, Mar. 3, 2020. URL: <https://appsso.eurostat.ec.europa.eu/nui/submitViewTableAction.do> (visited on 03/03/2020).
- [11] Luc van Nuffel. *The role of Trans-European gas infrastructure in the light of the 2050 decarbonisation targets: final report*. Rotterdam: Publications Office, Sept. 24, 2018. URL: <https://data.europa.eu/doi/10.2833/823109> (visited on 10/12/2021).
- [12] Martin Wietschel et al. *Metastudie Wasserstoff - Auswertung von Energiesystemstudien*. Metastudie. Karlsruhe, Freiburg, Cottbus: Fraunhofer-Institut für System- und Innovationsforschung ISI, Apr. 6, 2021, p. 87. URL: [https://www.wasserstoffrat.de/fileadmin/wasserstoffrat/media/Dokumente/Metastudie\\_Wasserstoff-Abschlussbericht.pdf](https://www.wasserstoffrat.de/fileadmin/wasserstoffrat/media/Dokumente/Metastudie_Wasserstoff-Abschlussbericht.pdf) (visited on 10/28/2021).

- [13] *Deutschland auf den Weg zur Klimaneutralität 2045 - Szenarien und Pfade im Modellvergleich*. Telegrafenberg: Potsdam-Institut für Klimafolgenforschung (PIK), 2021. URL: [https://ariadneprojekt.de/media/2021/10/Ariadne\\_Szenarienreport\\_Oktober2021-1.pdf](https://ariadneprojekt.de/media/2021/10/Ariadne_Szenarienreport_Oktober2021-1.pdf) (visited on 10/28/2021).
- [14] Ann-Katrin Lenz and Christoph Gatzert. *Wasserstoff zur Dekarbonisierung des Wärmesektors*. Studie. DVGW, June 29, 2021, p. 73.
- [15] Falko Ueckerdt et al. “Potential and risks of hydrogen-based e-fuels in climate change mitigation”. In: *Nature Climate Change* 11.5 (May 2021), pp. 384–393. ISSN: 1758-678X, 1758-6798. DOI: 10.1038/s41558-021-01032-7. URL: <http://www.nature.com/articles/s41558-021-01032-7> (visited on 11/12/2021).
- [16] European Parliament. *The European Green Deal*. 2019. URL: [https://www.europarl.europa.eu/doceo/document/TA-9-2020-0005\\_EN.pdf](https://www.europarl.europa.eu/doceo/document/TA-9-2020-0005_EN.pdf) (visited on 10/08/2021).
- [17] European Parliament, ed. *European Climate Law - Regulation*. June 30, 2021. URL: <https://eur-lex.europa.eu/legal-content/EN/TXT/PDF/?uri=CELEX:32021R1119&from=EN> (visited on 10/08/2021).
- [18] European Commission. *'Fit for 55': delivering the EU's 2030 Climate Target on the way to climate neutrality*. July 14, 2021. URL: <https://eur-lex.europa.eu/legal-content/EN/TXT/PDF/?uri=CELEX:52021DC0550&from=EN> (visited on 10/11/2021).
- [19] Panos Konstantin. *Praxisbuch Energiewirtschaft: Energieumwandlung, -transport und -beschaffung im liberalisierten Markt*. 3., aktual. Aufl. 2013. VDI-Buch. Berlin, Heidelberg: Springer Berlin Heidelberg, 2013. xviii+542. ISBN: 978-3-642-37265-0. DOI: 10.1007/978-3-642-37265-0. URL: <http://dx.doi.org/10.1007/978-3-642-37265-0> (visited on 03/18/2021).
- [20] William Greene and Laurits Christensen. “Economies of Scale in U.S. Electric Power Generation”. In: *Journal of Political Economy* 84 (Feb. 1, 1976), pp. 655–76. DOI: 10.1086/260470.
- [21] Georg Erdmann. *Energieökonomik: Theorie und Anwendungen*. In collab. with Peter Zweifel. 2., verb. Aufl.. Berlin [u.a.]: Springer, 2010. xx+376. ISBN: 978-3-642-12777-9.
- [22] Bundesministerium für Justiz und für Verbraucherschutz. *ARegV - Verordnung über die Anreizregulierung der Energieversorgungsnetze*. Oct. 29, 2007. URL: <https://www.gesetze-im-internet.de/aregv/BJNR252910007.html> (visited on 11/15/2021).
- [23] Daniel Then et al. “Analysis of Dependencies between Gas and Electricity Distribution Grid Planning and Building Energy Retrofit Decisions”. In: *Sustainability* 12.13 (Jan. 2020). Number: 13 Publisher: Multidisciplinary Digital Publishing Institute, p. 5315. DOI: 10.3390/su12135315. URL: <https://www.mdpi.com/2071-1050/12/13/5315> (visited on 03/08/2021).
- [24] A. J. Osiadacz. *Simulation and analysis of gas networks*. London: E. & F.N. Spon, 1987.
- [25] Benedikt Eberl and Julius Ott. “Entwicklung eines Dispatchmodells im Gasmarkt”. In: p. 10.
- [26] Daniel Lohmeier et al. “Pandapipes: An Open-Source Piping Grid Calculation Package for Multi-Energy Grid Simulations”. In: *Sustainability* 12.23 (Jan. 2020). Number: 23 Publisher: Multidisciplinary Digital Publishing Institute, p. 9899. DOI: 10.3390/su12239899. URL: <https://www.mdpi.com/2071-1050/12/23/9899> (visited on 03/08/2021).

- [27] Jonathan Chambers et al. “Mapping district heating potential under evolving thermal demand scenarios and technologies: A case study for Switzerland”. In: *Energy* 176 (June 2019), pp. 682–692. ISSN: 03605442. DOI: 10.1016/j.energy.2019.04.044. URL: <https://linkinghub.elsevier.com/retrieve/pii/S0360544219306681> (visited on 07/06/2021).
- [28] Prepared Simon Pezzutto et al. “D2.3 WP2 Report – Open Data Set for the EU28”. In: (Sept. 2019), p. 158.
- [29] J. C. Diettrich, A. Pluta, and W. Medjroubi. *SciGRID\_gas: The raw EMAP data set*. Germany: DLR Institute for Networked Energy System, July 22, 2020. URL: <https://www.gas.scigrd.de/>.
- [30] Andreas Müller and Marcus Hummel. *Hotmaps-Wiki - CM-Demand-Projection*. Oct. 2019. URL: <https://wiki.hotmaps.eu/en/CM-Demand-projection> (visited on 12/13/2021).
- [31] Lukas Kranzl and Andreas Müller. *Invert/EE-Lab*. Vienna: Vienna University of Technology, 2015. URL: <https://invert.at> (visited on 12/28/2021).
- [32] F. Pedregosa et al. “Scikit-learn: Machine Learning in Python”. In: *Journal of Machine Learning Research* 12 (2011), pp. 2825–2830.
- [33] Chire. *CC BY-SA 3.0 via Wikimedia Commons*. Oct. 20, 2011. URL: <https://creativecommons.org/licenses/by-sa/3.0>.
- [34] ENTSOG. *Maps — ENTSOG*. 2019. URL: <https://entsog.eu/maps#transmission-capacity-map-2019> (visited on 03/08/2021).
- [35] OpenStreetMap contributors. *Planet dump retrieved from https://planet.osm.org*. 2017. URL: <https://www.openstreetmap.org>.
- [36] Open Knowledge Foundation. *Open Data Commons Open Database License (ODbL)*. URL: <https://opendatacommons.org/licenses/odbl/> (visited on 11/08/2021).
- [37] Frederik Ramm et al. *GEOFABRIK*. Oct. 22, 2021. URL: <https://www.geofabrik.de/> (visited on 10/22/2021).
- [38] QGIS Development Team. *QGIS Geographic Information System*. 2009. URL: <http://qgis.org>.
- [39] F Sabo et al. *The European Settlement Map*. LU: Publications Office of the European Union, 2019. ISBN: 978-92-76-12184-8. URL: <https://data.europa.eu/doi/10.2760/25824> (visited on 12/14/2021).
- [40] E. Jones, T. Oliphant, P. Peterson, et al. *SciPy: open source scientific tools for Python*. 2015. URL: <http://www.scipy.org/> (visited on 11/08/2021).
- [41] Andrei Bocin et al. “JRC Open Power Plants Database (JRC-PPDB-OPEN)”. In: (July 3, 2019). Publisher: European Commission, Joint Research Centre (JRC). URL: <http://data.europa.eu/89h/9810feeb-f062-49cd-8e76-8d8cfd488a05> (visited on 10/22/2021).
- [42] Günter Cerbe and Deutsche Vereinigung des Gas- und Wasserfaches. *Grundlagen der Gastechnik: Gasbeschaffung, Gasverteilung, Gasverwendung*. 7., vollst. neu bearb. Aufl.. München Wien: Hanser, 2008. xxvi+627. ISBN: 978-3-446-41352-8.
- [43] fernbas. *EU Reference Scenario 2020*. Energy - European Commission. Feb. 10, 2019. URL: [https://ec.europa.eu/energy/data-analysis/energy-modelling/eu-reference-scenario-2020\\_en](https://ec.europa.eu/energy/data-analysis/energy-modelling/eu-reference-scenario-2020_en) (visited on 12/28/2021).

- [44] European Comission. *COMMISSION STAFF WORKING DOCUMENT EXECUTIVE SUMMARY OF THE IMPACT ASSESSMENT REPORT Accompanying the document COMMUNICATION FROM THE COMMISSION TO THE EUROPEAN PARLIAMENT, THE COUNCIL, THE EUROPEAN ECONOMIC AND SOCIAL COMMITTEE AND THE COMMITTEE OF THE REGIONS Stepping up Europe's 2030 climate ambition Investing in a climate-neutral future for the benefit of our people*. 2020. URL: <https://eur-lex.europa.eu/legal-content/EN/TXT/?uri=CELEX:52020SC0177> (visited on 12/28/2021).
- [45] Wiener Netze. *Kombinanzbetreiber - Wiener Netze GmbH*. 2020. URL: <http://www.wienernetze.at/kombinanzbetreiber> (visited on 01/06/2022).
- [46] Statistik Austria. *Energiebilanzen 2020*. Dec. 17, 2021. URL: [https://www.statistik.at/web\\_de/statistiken/energie\\_umwelt\\_innovation\\_mobilitaet/energie\\_und\\_umwelt/energie/energiebilanzen/index.html](https://www.statistik.at/web_de/statistiken/energie_umwelt_innovation_mobilitaet/energie_und_umwelt/energie/energiebilanzen/index.html) (visited on 01/06/2022).
- [47] Energie Graz. *Gas in Zahlen*. 2020. URL: <https://www.energie-graz.at/egg/unternehmen/geschafsbereiche/erdgas/erdgas-in-zahlen> (visited on 01/06/2022).
- [48] European Comission. *Database - Energy - Eurostat*. URL: <https://ec.europa.eu/eurostat/web/energy/data/database> (visited on 01/05/2022).